1
2

Reservoir Drawdown Highlights the Emergent Effects of Water Level Change on Reservoir Physics, Chemistry, and Biology

3 **Abigail S. L. Lewis[1], Adrienne Breef-Pilz[1], Dexter W. Howard[1], Mary E. Lofton[1], Freya**
4 **Olsson[1], Heather L. Wander[1], Cecelia E. Wood[2], Madeline E. Schreiber[2], Cayelan C.**
5 **Carey[1]**

6 [1] Department of Biological Sciences, Virginia Tech, Blacksburg, VA USA 24061

7 [2] Department of Geosciences, Virginia Tech, Blacksburg, VA USA 24061

8 Corresponding author: Abigail Lewis (aslewis@vt.edu)

9 **Key Points:**

10 • We monitored a small, eutrophic reservoir for two years to quantify the effects of a
11 month-long drawdown (36% reduction in reservoir volume)

12 • Coincident with drawdown, both stratification strength at the thermocline and epilimnetic
13 nutrient concentrations increased

14 • A subsequent cyanobacterial bloom led to decreased surface dissolved oxygen and
15 increases in solutes associated with bloom degradation

Abstract

Water level drawdowns are increasingly common in lakes and reservoirs worldwide as a result of both climate change and water management. Drawdowns can have direct effects on physical properties of a waterbody (e.g., by altering stratification and light dynamics), and can also have emergent effects on the waterbody's biology and chemistry. However, the emergent effects of drawdown remain poorly characterized in small, thermally-stratified reservoirs, which are common in the landscape. Here, we intensively monitored a small eutrophic reservoir for two years, including before, during, and after a month-long drawdown that reduced total reservoir volume by 36%. Our study aimed to quantify the effects of water level change on reservoir physical, chemical, and biological properties. During drawdown, stratification strength (maximum buoyancy frequency) and surface phosphate concentrations both increased, contributing to a substantial surface phytoplankton bloom. The peak in phytoplankton biomass was followed by cascading changes in surface water chemistry, with sequential peaks in dissolved organic carbon, dissolved carbon dioxide, and ammonium concentrations that reflect biogeochemical processes associated with bloom degradation. Dissolved oxygen concentrations substantially decreased in the surface waters during drawdown (to 41% saturation), which was associated with increased iron and manganese concentrations. Combined, our results illustrate how changes in water level can have emergent effects on coupled physical, chemical, and biological processes. As climate change and water management continue to increase the frequency of drawdowns in lakes worldwide, our results highlight the importance of characterizing how water level variability can alter complex in-lake ecosystem processes, thereby affecting water quality.

Plain Language Summary

Changes in climate and water management are having substantial effects on the water level of lakes and reservoirs around the world. In particular, the frequency with which waterbodies experience water level drawdowns is increasing worldwide. However, the effects of drawdown on aquatic physics, chemistry, and biology remain poorly understood. Here, we intensively monitored before, during, and after a drawdown in Beaverdam Reservoir, VA, USA, during which water volume decreased by 36% over the course of one month. Physical changes to the waterbody during drawdown led to increased nutrient concentrations in surface water, which contributed to the formation of a substantial phytoplankton bloom. Degradation of the phytoplankton bloom then resulted in decreased dissolved oxygen and increased dissolved carbon dioxide in surface waters, among other chemical changes. Combined, our results illustrate how changes in water level can have cascading effects on coupled physical, chemical, and biological processes in lakes. As drawdowns become increasingly common in lakes and reservoirs worldwide, our results highlight the effects of water level variability on interconnected aquatic processes, with important implications for water quality worldwide.

1 Introduction

Water levels in many lakes and reservoirs are changing due to altered climate and water management practices (Kraemer et al., 2020; Wada et al., 2014; Ye et al., 2017). While global climate change is driving a general trend of decreasing water levels in lakes and reservoirs (Fergus et al., 2022; Yao et al., 2023), local human activities also cause short-term water level changes (e.g., Furey et al., 2004; Hannoun & Tietjen, 2023; Liu et al., 2019; Rimmer et al.,

59 2011). In particular, many human-made reservoirs experience large water level fluctuations on
60 daily to annual timescales due to management for flood control, hydropower, irrigation, and
61 drinking water provision (Fergus et al., 2022; Jiang et al., 2018; Keller et al., 2021; Wada et al.,
62 2014). The seasonal variability of water level in managed reservoirs is, on average, more than
63 four times greater than in natural waterbodies (Cooley et al., 2021), and extreme, non-seasonal
64 water level fluctuations may also be more common in these managed systems. As just one
65 example, water level fluctuated by ~50 m over two years in Lake Shasta, a reservoir in
66 California, USA (Zohary and Ostrovsky 2011). As the frequency of water level drawdowns
67 increases due to both climate change and water management (Cooley et al., 2021; Kraemer et al.,
68 2020; Ye et al., 2017; Zhao et al., 2022), it is critical to determine the ecosystem-level effects of
69 water level change on the interconnected biological, chemical, and physical processes that shape
70 water quality.

71   Decreases in water level can play an important role in structuring reservoir physical
72 dynamics. Depending on the depth of water extraction, reservoirs may differentially lose volume
73 from the epilimnion (the warmer surface water layer) or the hypolimnion (the colder bottom
74 water layer), which could mediate the effects of drawdown on reservoir heat budgets, thermal
75 stratification, and water quality (Nürnberg, 2007; Zohary & Ostrovsky, 2011). Decreased
76 hypolimnetic volume may result in a warmer overall waterbody, weaker thermal stratification,
77 and a proportionally smaller anoxic (<1 mg/L dissolved oxygen) volume in the reservoir
78 (Barbiero et al., 1997; Li et al., 2017; Nürnberg, 2007, 2020), while decreased epilimnetic
79 volume may result in a colder waterbody, stronger thermal stratification, and a proportionally
80 greater volume of anoxic water (Barbiero et al., 1997; Li et al., 2017; Moreno-Ostos et al., 2008;
81 Wang et al., 2012). Stratification strength may further be altered by changes in the light
82 environment of a reservoir during drawdown. For example, increased light penetration to the
83 sediments due to reduced water depth may result in increased hypolimnetic warming (Matsuzaki
84 et al., 2023). Conversely, increased epilimnetic turbidity resulting from drawdown-induced
85 littoral erosion may increase surface warming and decrease hypolimnetic temperatures (Jones et
86 al., 2005; Kumagai et al., 2000). Across drawdowns, decreased water volume will be expected to
87 decrease the resistance to full water column mixing (Wetzel, 2001), though the occurrence of
88 mixing events and consequent effects on water quality will depend on the magnitude of
89 drawdown and initial thermal stability of the reservoir. Ultimately, the responses of light
90 conditions and thermal structure to drawdown is likely to differ in reservoirs of varying
91 morphometry, which is a key driver of thermal stratification dynamics (Butcher et al., 2015;
92 Kraemer et al., 2015; Magee & Wu, 2017), making the net effect of drawdown on stratification
93 strength challenging to predict (Figure 1a).

94   Changes in reservoir physical properties due to drawdown may cascade to alter chemical
95 and biological dynamics, but the net effects of multiple interacting ecosystem processes remain
96 unresolved (Figure 1). If hypolimnetic water is withdrawn from the reservoir (e.g., for water
97 quality management or downstream temperature regulation), nutrient and metal concentrations
98 may decrease at the whole-ecosystem scale (Nürnberg, 2007, 2020). However, if epilimnetic
99 water is withdrawn (e.g., for some drinking water, irrigation, and hydroelectric purposes), or if
100 hypolimnetic withdrawal weakens thermal stratification, epilimnetic nutrients may increase as a
101 result of increased entrainment from the hypolimnion (Zohary & Ostrovsky, 2011). Furthermore,
102 littoral erosion and sediment drying due to water level fluctuations may lead to inputs of nitrogen
103 (N), phosphorus (P), and carbon (C) from littoral sediments, increasing surface concentrations
104 during drawdown (Klotz & Linn, 2001). Increased nutrient concentrations can subsequently lead

105 to increased phytoplankton biomass (e.g., Baldwin et al., 2008; Naselli-Flores & Barone, 2005).
106 However, the effect of increased nutrient concentrations could be tempered by expected declines
107 in light availability resulting from increased turbidity (e.g., Perrin et al., 2000). Taken together,
108 these divergent changes in nutrient and light availability could result in positive or negative net
109 effects on total phytoplankton biomass (Ma et al., 2023; Figure 1b). Moreover, alteration of
110 thermal stratification by drawdown could also alter the distribution of phytoplankton biomass
111 throughout the water column (Leach et al., 2018; Lofton et al., 2020, 2022). Drawdown could
112 alter biomass distributions either by inducing mixing, thereby homogenizing biomass across
113 depths (Kasprzak et al., 2017; Planas & Paquet, 2016; Rinke et al., 2009; Wu et al., 2015), or by
114 facilitating the formation of deep maxima of biomass if thermal stratification increases post-
115 drawdown (Alldredge et al., 2002; Cullen, 2015; Lewis et al., 2017).

116   Among freshwater ecosystem variables, the net effect of drawdown on dissolved oxygen
117 (DO) concentrations is particularly difficult to predict, as DO is modulated by interacting
118 physical (e.g., stratification dynamics), chemical (e.g., oxygen demand by reduced solutes), and
119 biological conditions (e.g., production and respiration; Figure 1c). DO may increase in surface
120 waters if primary productivity increases, or decrease if primary productivity decreases (Odum,
121 1956). Likewise, decomposition of phytoplankton biomass and inputs of allochthonous organic
122 carbon due to littoral erosion could potentially stimulate epilimnetic respiration, thereby
123 decreasing DO concentrations and increasing the production and emission of carbon dioxide
124 (CO_2) and methane (CH_4), as has been observed in other freshwater drawdown studies (Amani et
125 al., 2022; Beaulieu et al., 2018; Harrison et al., 2017; Kosten et al., 2018). Decreased
126 stratification strength could cause whole-ecosystem DO concentrations to increase with mixing
127 of well-oxygenated surface waters into the hypolimnion, or loss of oxic epilimnetic water from
128 the reservoir could cause whole-ecosystem DO concentrations to decrease (e.g., Matsuzaki et al.,
129 2023). Depending on the direction and magnitude of change in DO, further cascading effects on
130 other ecosystem processes (e.g., dissolved metals concentrations, greenhouse gas production,
131 etc.) may be expected. Overall, while the effects of drawdown on reservoir physics, chemistry,
132 and biology are increasingly being examined (e.g., Deemer & Harrison, 2019; Matsuzaki et al.,
133 2023), less is known about the emergent responses to drawdown that arise from changes in
134 multiple, interconnected ecosystem processes (Figure 1).

135   The ecosystem-level effects of drawdowns are particularly unresolved in small,
136 thermally-stratified waterbodies, which are common in the landscape (Downing et al., 2006). In
137 the United States, over 90% of reservoirs are less than 1 km^2 in surface area (Figure S1; U.S.
138 Army Corps of Engineers, 2021). However, previous whole-ecosystem studies examining the
139 effects of water level changes have often focused on large lakes and reservoirs (e.g., Nakanishi et
140 al., 2022; Ouyang et al., 2021; Table S1) or very shallow, weakly-stratified or fully-mixed
141 waterbodies (e.g., Coops et al., 2003; Matsuzaki et al., 2023; Table S1). Other studies have been
142 conducted in mesocosms that cannot encompass all interacting factors occurring on a whole-
143 ecosystem scale (e.g., Matsuzaki et al., 2023). Moreover, much of the existing literature
144 examining the whole-ecosystem effects of water level drawdown has focused on seasonal or
145 drought-induced changes (see Table S1), which co-occur with changes in temperature and
146 precipitation. Thus, as opportunities to perturb whole ecosystems and examine the couplings
147 between lake and reservoir physics, chemistry, and biology are rare (Barley & Meeuwig, 2017),
148 management-driven drawdowns provide an excellent opportunity for whole-ecosystem
149 experimentation.

150   Here, we intensively monitored a month-long drawdown in a small eutrophic reservoir to
151   analyze the emergent effects of water level change on reservoir physics, chemistry, and biology
152   (Figure 1). Specifically, our study aimed to assess the effects of drawdown on three focal
153   variables: thermal stratification strength, phytoplankton biomass and depth distribution, and DO
154   concentrations. We expected that changes in these three focal variables would be mediated by
155   concurrent changes in water temperature, light penetration, and nutrient concentrations that result
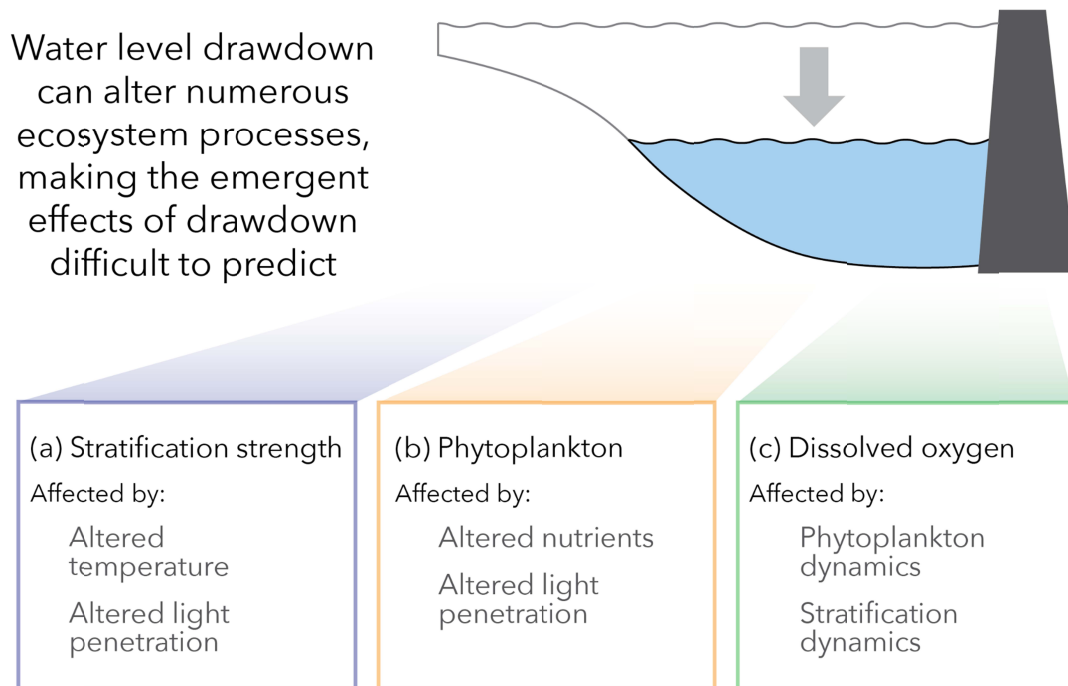156   from multiple ecosystem interactions during drawdown (Figure 1).

157

158

159   **Figure 1:** Hypothesized emergent responses of (a) thermal stratification strength, (b)
160   phytoplankton biomass and depth distribution, and (c) dissolved oxygen concentrations to water
161   level drawdown, with predominant drivers. Note that the timeline of responses is likely to differ
162   among emergent responses.

163   **2 Methods**

164   2.1 Study site

165   Beaverdam Reservoir is a small, dimictic reservoir located in Vinton, Virginia, USA
166   (37.3128° N, 79.8160° W; Figure 2) that is owned and operated as a secondary drinking water
167   source by the Western Virginia Water Authority. When the reservoir is at full pond it has a
168   maximum depth of 13.4 m, surface area of 0.39 km^2, and residence time of ~0.9 y (Hamre et al.,
169   2018). The catchment area of the reservoir is 3.69 km^2, and consists primarily of deciduous
170   forest (Hamre et al., 2018). The reservoir is typically thermally stratified from May through
171   October, and experiences hypolimnetic anoxia throughout the summer stratified period (Doubek
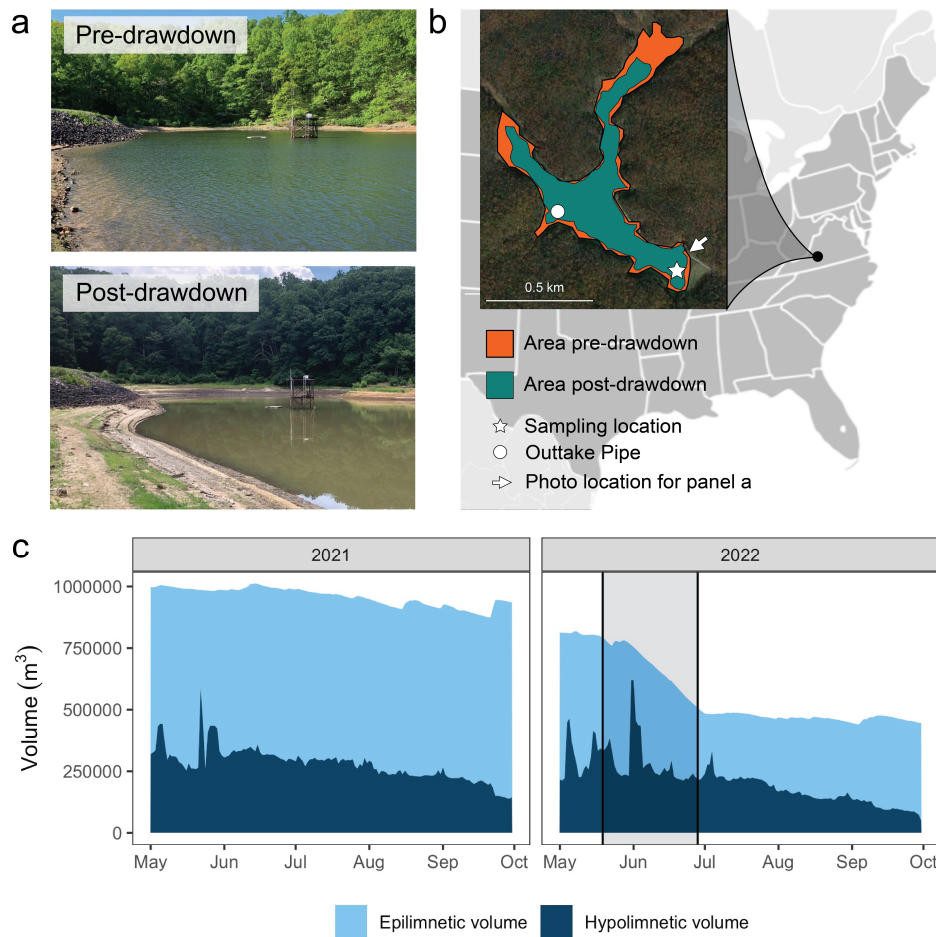172   et al., 2018).

173

174
Figure 2: A drawdown in summer 2022 substantially decreased water level in Beaverdam
Reservoir. (a) Photos of the reservoir before (top, 9 May 2022) and after (bottom, 5 July 2022)
the month-long drawdown. (b) The spatial extent of the reservoir surface area change from pre-
drawdown in May (orange) to post-drawdown in July (teal), traced from satellite imagery. The
background map shows the location of the reservoir within North America. (c) Change in
epilimnetic and hypolimnetic water volume in 2021 and 2022. Vertical lines indicate when the
outtake pipe was opened and closed, with the shaded month noting the drawdown interval.

2.2 Water level drawdown (2022) and reference year (2021)

We monitored water physics, chemistry, and biology in Beaverdam Reservoir for two
years (2021–2022), which included a reference year prior to the drawdown in 2022. During the
reference year (2021), water level was higher than in 2022 ($\mu = 10.7 \pm 0.4$ m SD) and relatively
constant throughout the stratified period. On 19 May 2022, managers opened an outtake pipe
(see Figure 2b) at Beaverdam Reservoir to lower water level for dam maintenance. At the time
that the drawdown began, the maximum depth of the reservoir was 10.1 m. The outtake pipe is in
a shallower area of the reservoir and was in the epilimnion throughout a majority of the
drawdown period (Figure 3a). Due to precipitation in the days following 19 May, water level did
not begin to decline until several days after the pipe was opened (approximately 28 May; Figure
2c). The outtake pipe was closed on 28 June 2022. Following 28 June 2022, water level stayed

193 relatively constant throughout the remainder of the summer stratified period ($\mu = 7.9 \pm 0.1$ m),
194 then increased gradually throughout the fall and winter.

195   2.3 Monitoring program

196   2.3.1 *In situ* sensors

197   We used a suite of high-frequency *in situ* sensors to continuously monitor water level and
198 water temperature at the deepest site of the reservoir near the dam (Figure 2b). A Campbell
199 Scientific pressure transducer (Logan, UT, USA) was fixed at 0.2 m above the sediments, and
200 NexSens T-Node FR Temperature Sensor thermistors (NexSens, Fairborn, OH, USA) were
201 deployed at 1 m intervals from 0.2 m above the sediments to 13.2 m above the sediments. Both
202 the pressure transducer and temperature sensors were affixed to a metal platform and therefore
203 did not move up or down in absolute elevation as the water level changed in the reservoir (see
204 Carey et al., 2023c).

205   In addition to the in-water sensors, we also measured air temperature, wind speed, and
206 precipitation using a research-grade Campbell Scientific meteorological station that collected
207 data every minute (Carey & Breef-Pilz, 2023). The station was located at 37.3027º N, 79.8369º
208 W, 2.17 km from the sampling site at Beaverdam Reservoir. Air temperature was measured
209 using a HC2S3 Temperature and Relative Humidity probe by Rotronic Instrument Corp
210 (Hauppauge, NY, USA). Wind speed was measured using a R.M. Young Wind Monitor Model
211 05103 (RM Young Company, Traverse City, MI, USA), which averaged wind speeds over the
212 minute. Precipitation was measured using a TE525WS-L Rain Gage (Texas Electronics Inc.,
213 Dallas, TX, USA), which measures rainfall in 0.254 mm increments (Carey & Breef-Pilz, 2023).

214   2.3.2 Field sampling

215   To complement *in situ* sensor data, we measured a suite of water quality variables weekly
216 or fortnightly throughout the duration of this two-year study. Field sampling methods involved
217 both manual sensor profiles and grab samples at multiple depths.

218   2.3.2.1 Sensor profiles

219   Full water-column profiles of DO (concentration and percent saturation),
220 photosynthetically active radiation (PAR), and turbidity were collected using a SeaBird 19plus
221 V2 SeaCAT Profiler Conductivity, Temperature, and Depth (CTD) profiler (Sea-Bird Scientific,
222 Bellevue, WA, USA). These profiles were collected approximately weekly during the summer
223 stratified periods of 2021 and 2022, and monthly during the fall, winter, and spring. A YSI
224 ProODO Optical Dissolved Oxygen Instrument (YSI Inc., Yellow Springs, OH, USA) was used
225 to record DO concentrations at 1 m depth intervals in the reservoir from July - December 2021
226 during CTD maintenance; a comparison of the CTD and YSI DO sensors shows very strong
227 correspondence (Carey et al., 2022a).

228   We used a FluoroProbe (bbe Moldaenke, Schwentinental, Germany) to measure
229 phytoplankton biomass and depth distribution in the reservoir. FluoroProbes are submersible, *in-*
230 *situ* fluorometers that estimate biomass of four spectral groups using fluorescence of a suite of
231 photosynthetic pigments (Catherine et al., 2012; Kring et al., 2014): (1) green algae, which is
232 largely correlated with chlorophyll-*a* and chlorophyll-*b* fluorescence; (2) cyanobacteria
233 (phycocyanin); (3) brown algae (xanthophyll, fucoxanthin, and peridinin); and (4) cryptophytes

234   or mixed algae (phycoerythrin; Beutler et al., 2002). Biomass of the four spectral groups at each
235   measured depth was then summed to produce depth-specific total phytoplankton biomass
236   concentrations (Carey et al., 2023d).

237   *2.3.2.2 Water chemistry grab samples*

238   We used a 4-L Van Dorn sampler (Wildco, Yulee, FL, USA) to collect water chemistry
239   samples at 0.1, 3, 6, 9, and 10 m. If the water level was too low to obtain a 9 m or 10 m sample,
240   we collected samples to all of the routine monitoring depths possible and also from ~1 m above
241   the sediments. At each depth, subsamples were taken for dissolved greenhouse gases, dissolved
242   organic carbon (DOC), total and soluble N and P, and total and soluble iron (Fe) and manganese
243   (Mn) concentrations.

244   Water samples for dissolved carbon dioxide (CO_2) were collected from the Van Dorn
245   sampler and immediately sealed in 20-mL glass vials with crimped septum caps and no
246   headspace. These samples were kept on ice, then refrigerated in the lab and analyzed within 24
247   hr (Carey et al., 2023b).

248   Samples for DOC and total and soluble N and P were collected in acid-washed
249   polypropylene bottles. Unfiltered water samples were used for analysis of total nitrogen (TN)
250   and total phosphorus (TP). Filtered water samples (Thomas Scientific GF/F 0.7 μm filters) were
251   collected for analysis of DOC, ammonium (NH_4^+), nitrate (NO_3^-), and soluble reactive
252   phosphorus (SRP). Both total and filtered nutrient and C samples were frozen for later analysis,
253   as described below (Carey et al., 2023e).

254   Water samples for analysis of Fe and Mn were collected in 15-mL centrifuge tubes.
255   Unfiltered samples were analyzed for total Fe and Mn. A separate aliquot was filtered
256   immediately upon collection with a 0.45-μm nylon membrane for analysis of soluble Fe and Mn.
257   Samples for metals analysis were preserved with trace metal grade nitric acid in the field to pH
258   <2 (Schreiber et al., 2023).

259   2.4 Laboratory analysis

260   2.4.1 Greenhouse Gases

261   Dissolved CO_2 concentrations were measured on a Shimadzu Nexis GC-2030 Gas
262   Chromatograph (GC; Shimadzu, Kyoto, Japan) with a Flame Ionization Detector (FID) and
263   Thermal Conductivity Detector (TCD) following McClure et al. (2018). Prior to analysis, a 2-mL
264   headspace was created with Helium (He) by displacing 2-mL of sample water and equilibrated
265   by shaking each sample at 300 rpm for 15 minutes. The 2-mL headspace was then injected into
266   the GC at a temperature of 35 degrees C and a carrier gas (He) flow rate of 15 mL/min.
267   Dissolved concentrations of CO_2 in water were calculated using the observed head-space
268   concentrations and Henry's Law (Carey et al., 2023b; McClure et al., 2018).

269   2.4.2 Carbon, nitrogen, and phosphorus

270   Water column depth profiles of C, N, and P concentrations were measured following
271   collection in the field. DOC samples were poured into glass vials which had been acid-washed
272   and combusted at 550°C. These samples were analyzed on an Elementar vario TOC cube
273   (Elementar Analysensysteme GmbH, Hanau, Germany) using the persulfate catalytic method

274 (Brenton & Arnett, 1993). The detection limit for DOC was 0.76 mg/L. Samples for NH_4^+, NO_3^-,
275 and SRP were analyzed colorimetrically using flow injection analysis (APHA 2005) on a Lachat
276 Instruments XYZ Autosampler ASX 520 Series and QuikChem Series 8500 (Lachat ASX 520
277 Series, Lachat Instruments, Loveland, Colorado, USA). Method detection limits were 4.3 µg/L
278 (NH_4^+), 3.8 µg/L (NO_3^-), and 3.0 µg/L (SRP), determined following Carey et al. (2023e).
279 Samples for TN and TP were digested with alkaline persulfate and then analyzed
280 colorimetrically using flow injection analysis. Method detection limits were 56 µg/L (TN) and
281 3.5 µg/L (TP). Additional analytical methodology can be found in the data publication (Carey et
282 al., 2023e).

283   2.4.3 Fe and Mn

284   Samples for total and soluble Fe and Mn were analyzed by ICPMS (inductively coupled
285 plasma mass spectrometry; Thermo Electron iCAP RQ). Detection limits were 0.80 µg/L (Fe)
286 and 0.004 µg/L (Mn).

287   2.5 Data analysis

288   2.5.1 Thermal Stratification

289   We calculated multiple metrics to quantify how thermal conditions changed in
290 Beaverdam Reservoir following drawdown. Schmidt stability (Idso, 1973), a measure of total
291 water column stability; maximum buoyancy frequency, a measure of local stability at the
292 thermocline; and thermocline depth were calculated using the R package *rLakeAnalyzer* (Read et
293 al., 2011) using *in situ* high-frequency thermistor data. Thermocline depth was calculated using a
294 minimum density difference of 0.1 kg/m^3 (Lewis et al., 2023; following Wilson et al., 2020). For
295 simplicity, we refer to all volume above the thermocline as the epilimnion and all volume below
296 the thermocline as the hypolimnion. Schmidt stability was calculated with dynamic bathymetry
297 as the reservoir volume changed during drawdown by updating the depth of each hypsometric
298 layer of the reservoir with daily water level data (Lewis et al., 2023). We determined the date of
299 fall turnover as the first day surface and bottom temperatures were within 1 ºC, following
300 McClure et al. (2020).

301   2.5.2 Phytoplankton depth distribution metrics

302   We calculated two metrics from the FluoroProbe data to characterize the depth
303 distributions of fluorescence-based phytoplankton biomass in Beaverdam Reservoir following
304 Lofton et al. (2020, 2022). First, we calculated the chlorophyll maximum (C_{max}) depth as the
305 depth at which the maximum concentration of fluorescence-based biomass of each spectral group
306 (green algae, brown algae, cyanobacteria, mixed algae, and total phytoplankton) was observed.
307 Second, we calculated the width of the biomass peak (peak width) for each spectral group and
308 for total phytoplankton biomass. To determine peak width, we identified the depths above and
309 below the maximum observed biomass where observed biomass was nearest to the mean
310 biomass concentration across the water column. The distance between these two depths in meters
311 was assigned as the peak width (see Figure S2). While we calculated C_{max} depth and peak width
312 for all four spectral groups and total phytoplankton, we focus our reporting on fluorescence-
313 based biomass of cyanobacteria and total phytoplankton, as cyanobacteria exhibited the highest
314 biomass concentrations of any spectral group on 64% of $n = 25$ total sampling days between 1
315 May–1 September in 2021 and 2022.

3 Results

Water level changed substantially during drawdown, altering Beaverdam Reservoir's physics, chemistry, and biology. From the beginning (19 May) to the end (28 June) of the 2022 drawdown, the total volume of Beaverdam Reservoir decreased by 36% (from 795,000 m^3 to 508,000 m^3; Figure 2c). In comparison, during the same time period in the reference year (2021), water volume increased by 0.2% (from 989,000 m^3 to 991,000 m^3) due to seasonal fluctuations in the reservoir's water budget (Figure 2c). Drawdown resulted in a loss of 69,000 m^2 of reservoir surface area and reduced maximum reservoir depth by 1.7 m, from 10.4 m to 8.7 m (Figure 2a, 2b).

Due to epilimnetic water extraction, the majority (61%) of the observed change in the reservoir's volume during the drawdown resulted from a loss of epilimnetic water (Figure 2c, Figure 3a). Total epilimnetic volume decreased by 37% (from 462,000 m^3 to 290,000 m^3). Disproportionate loss of warm epilimnetic water resulted in a 2.6 ºC decrease in mean volume-weighted temperature of the reservoir in 2022 compared to 2021 during the month following drawdown (July 2021: 23.1 ± 0.6 ºC; July 2022: 20.5 ± 0.8 ºC; Figure 4c).
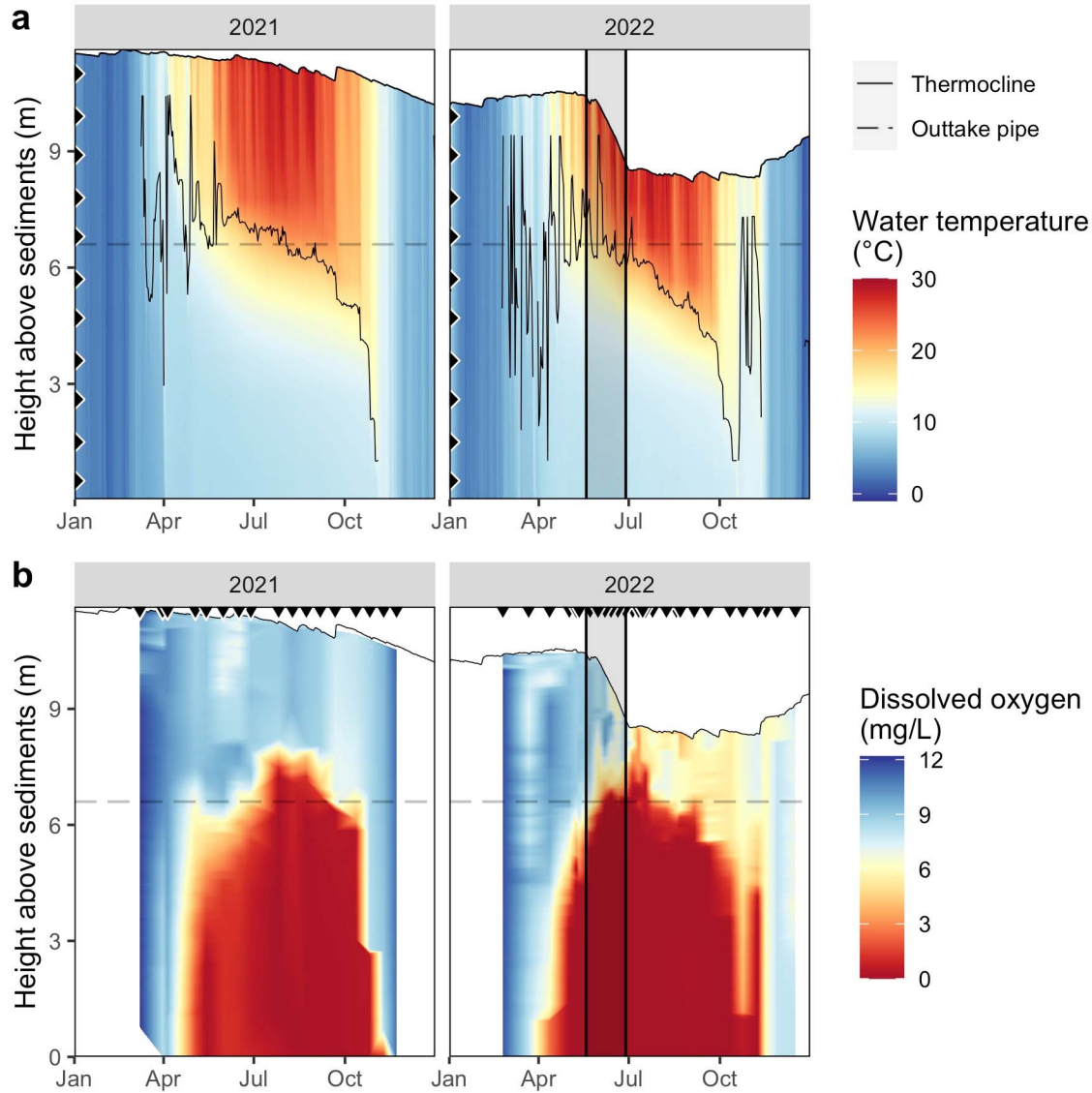
Figure 3: Drawdown decreased epilimnion thickness and increased the anoxic (i.e., dissolved oxygen concentration <1 mg/L) proportion of the water column in 2022 at Beaverdam Reservoir. (a) Heatmap of water temperature measured with *in-situ* thermistor sensors throughout 2021 and 2022, with the thermocline depth indicated by a solid black line. Ticks at the left of each panel indicate sensor depths. (b) Heatmap of dissolved oxygen concentrations sampled using CTD sensor profiles in 2021 and 2022. Ticks at the top of the figure indicate CTD sampling dates. We interpolated among sensor depths (panel a) and sampling dates (panel b) to create the heatmaps. Shaded interval indicates the 2022 drawdown period in both panels. The depth of the outtake pipe that was opened in 2022 is marked using a dashed line.
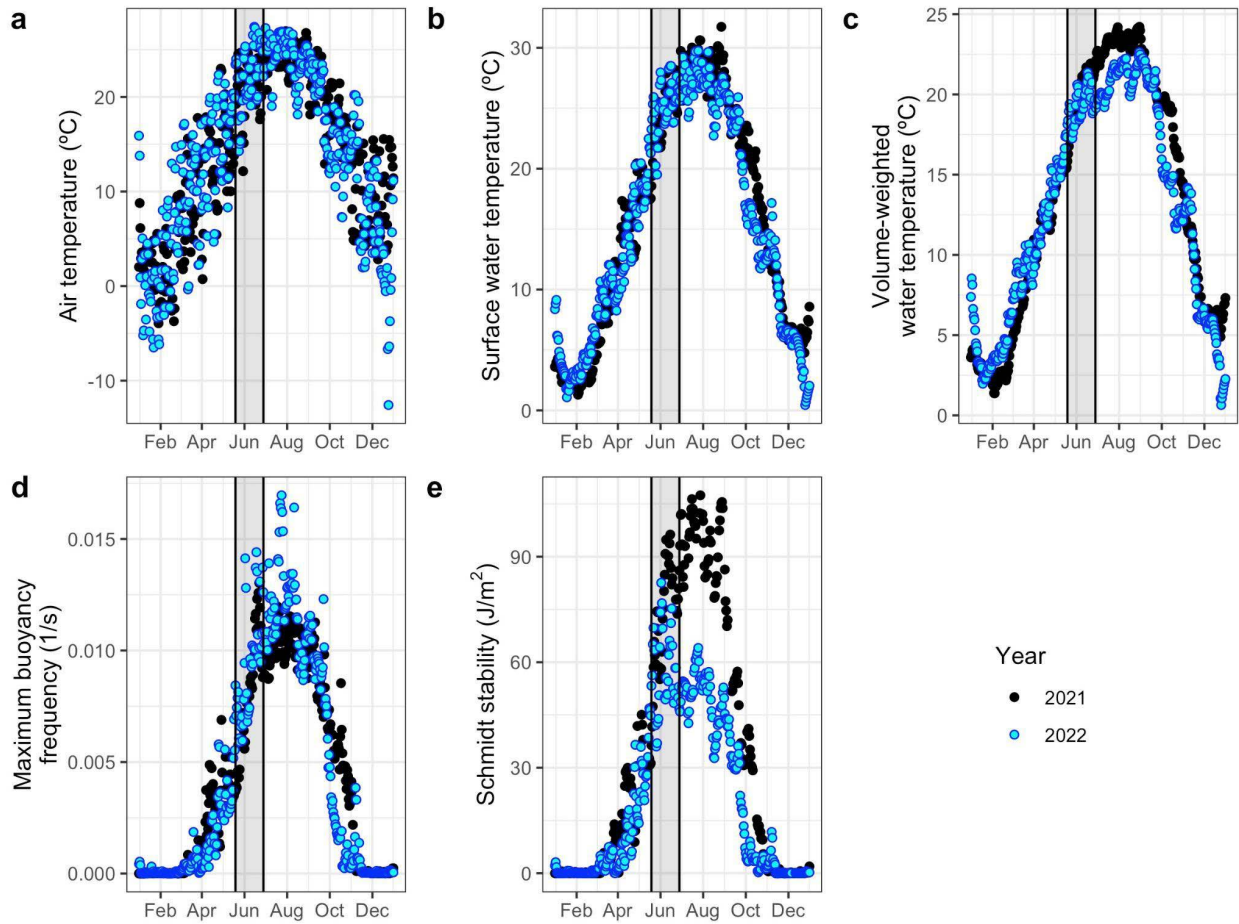
Figure 4: Air temperatures (a) and surface water temperatures (b) were similar between 2021 and 2022. Conversely, drawdown was associated with decreased volume-weighted water temperature of the entire reservoir (c), increased maximum buoyancy frequency (d), and decreased Schmidt stability (e) in 2022, compared to 2021. Shaded intervals indicate the 2022 drawdown period.

Meteorological conditions were similar between the reference and drawdown years. Mean air temperature was 21.3 ± 4.2 ºC (± 1 S.D.) between 19 May and 28 June in 2021 and 22.1 ± 4.9 ºC during the same interval in 2022 (Figure 4a). Likewise, wind speeds were similar between the two years, with a mean of 1.7 ± 1.1 m/s between 19 May and 28 June in 2021 and 1.9 ± 1.4 m/s during the same interval in 2022 (Figure S3b). Total precipitation was slightly greater in 2022 than in 2021, particularly during the first several days of drawdown (Figure S3a). Mean daily precipitation was 0.8 ± 2.9 mm between 19 May and 28 June in 2021 and 4.2 ± 8.7 mm during the same interval in 2022, though mean daily precipitation was similar between the two years (2.3 ± 7.1 mm/d in 2021, 3.4 ± 8.1 mm/d in 2022; Figure S3a).

3.1 Stratification strength

Maximum buoyancy frequency and Schmidt stability responded in contrasting ways to reservoir drawdown. While July buoyancy frequency was 25% higher in 2022 (0.013 ± 0.002 1/s) than in 2021 (0.010 ± 0.001 1/s), Schmidt stability plateaued immediately after the start of

361 drawdown, resulting in 44% lower Schmidt stability values in July 2022 (54 ± 5 J/m^2) relative to
362 July 2021 (97 ± 7 J/m^2; Figure 4d, 4e). Correspondingly, fall turnover was 18 days earlier in
363 2022 (19 October) relative to 2021 (6 November).

364   3.2 Phytoplankton and biogeochemical dynamics

365   Water level drawdown was associated with substantial changes in the magnitude and
366 timing of reservoir biogeochemistry and phytoplankton dynamics. In 2022, surface water TN,
367 TP, phytoplankton biomass, DOC, dissolved CO_2, and NH_4^+ all exhibited concentrations
368 substantially higher than the range of conditions observed in 2021 (Figure 5). Peaks of TP, TN,
369 and phytoplankton biomass on 27 June were preceded by a peak in SRP on 20 June. Surface
370 water DOC concentrations peaked 8 days after phytoplankton (5 July), followed by peaks in
371 dissolved CO_2 (11 July) and NH_4^+ (18 July). A comparison of maximum concentrations between
372 the two years reveals that in 2022 (vs. 2021), peak TP concentrations were 77% higher (by 15.1
373 µg/L), TN concentrations were 271% higher (by 1059 µg/L), phytoplankton concentrations were
374 147% higher (by 29.5 µg/L), DOC concentrations were 177% higher (by 6.9 µg/L), dissolved
375 CO_2 concentrations were 257% higher (by 43 µmol/L), and NH_4^+ concentrations were 2273%
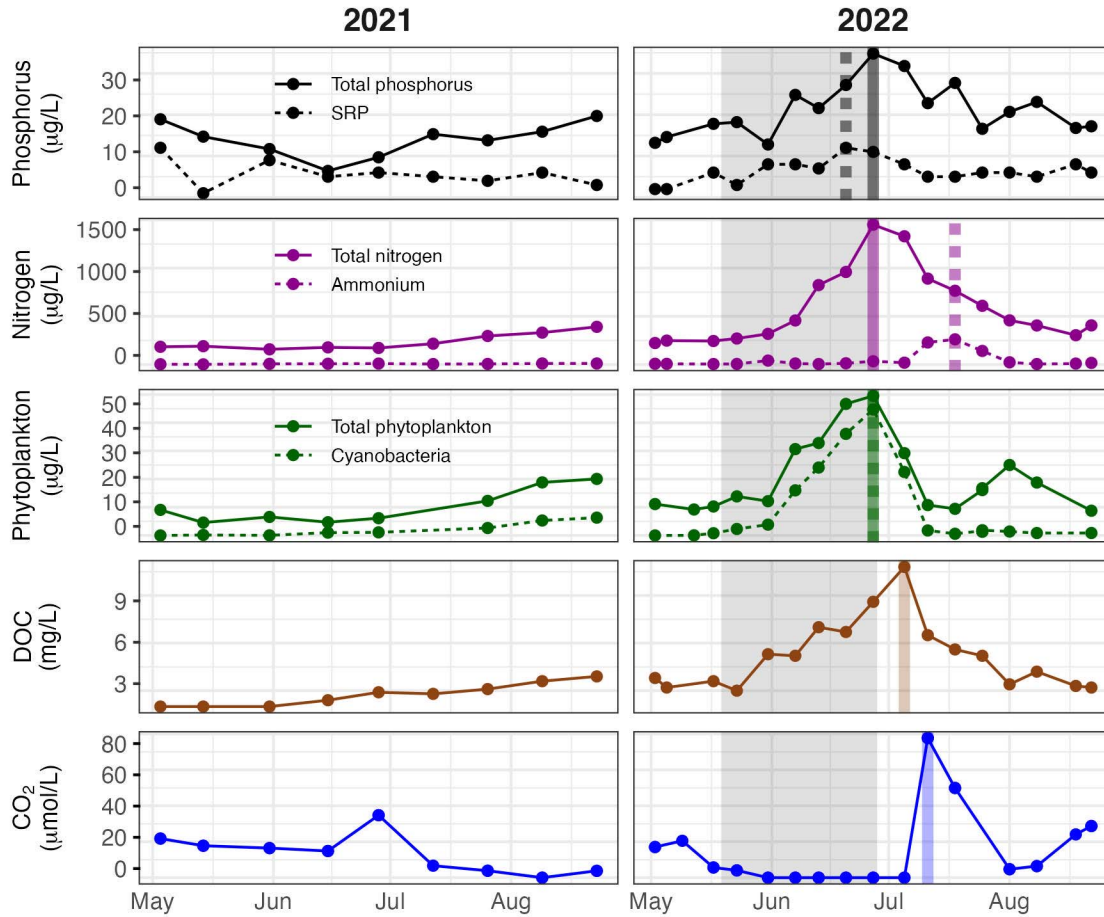376 higher (by 250 µg/L) than in 2021 (Figure 5).
377

Figure 5: Time series of select water chemistry and biological variables at 0.1 m depth in Beaverdam Reservoir during summers 2021 (left panels) and 2022 (right panels). A June 2022 peak in surface soluble reactive phosphorus (SRP) was followed by peaks in total phosphorus, total nitrogen, phytoplankton, and cyanobacteria. Dissolved organic carbon (DOC) peaked 8 days later, followed by a peak in dissolved carbon dioxide (CO_2), and finally a peak in ammonium. Colored vertical lines indicate the timing of the observed maximum concentration for each variable in 2022. Points represent discrete sampling visits. Grey shading indicates the drawdown period in 2022.

Changes in the underwater light environment due to drawdown altered depth distributions of phytoplankton biomass across the water column. Turbidity increased sharply following the onset of drawdown in 2022, with a peak 1100% higher than the maximum observed turbidity in 2021 (24.7 NTU higher; Figure 6). Coincident with this peak, the euphotic zone depth (defined as 1% of surface light) reached a minimum value of 1.5 m, which was 2.9 m shallower than the shallowest euphotic zone depth observed in 2021. The depth of maximum phytoplankton biomass was shallower and peak widths were narrower for both total biomass and cyanobacteria during the drawdown in 2022 than in 2021. In 2022, the shallowest C_{max} depth for cyanobacteria coincided with the date of maximum turbidity (5 July, just after the drawdown ended), while the shallowest C_{max} depth for total phytoplankton and the narrowest peak width for both total phytoplankton and cyanobacteria occurred mid-drawdown, 2–3 weeks earlier (Figure 6).
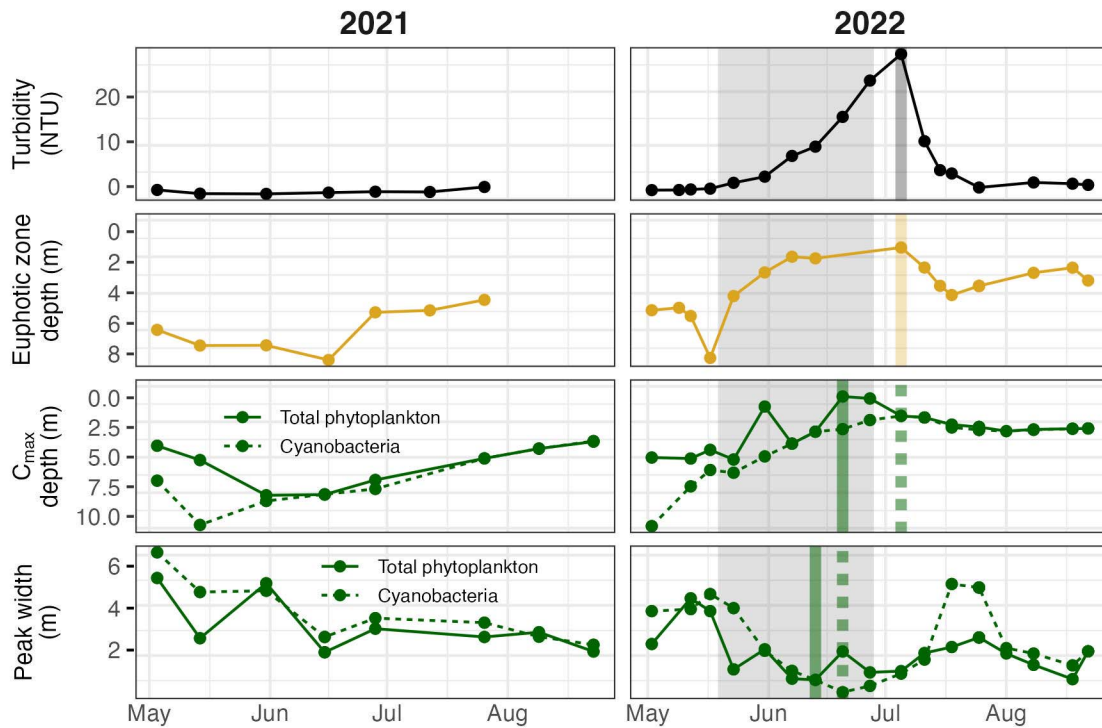
398

399

Figure 6: Turbidity peaked and euphotic zone depth was shallowest just after the drawdown at
Beaverdam Reservoir in 2022. C_{max} depth and peak width of total phytoplankton (solid) and
cyanobacteria (dotted) also reached a minimum on or before this date. Colored vertical lines
indicate observed maxima (Turbidity) or minima (Euphotic zone depth, Total phytoplankton and
Cyanobacteria C_{max} depth and Peak width) for each variable in 2022. Points represent discrete
sampling visits. Gray shading indicates the drawdown period in 2022. Note reversed y-axes for
euphotic zone depth and C_{max} depth, with 0 m corresponding to the reservoir surface.

3.3 Dissolved oxygen

Both surface DO concentrations and depth-resolved DO profiles differed substantially
before and after drawdown, which was associated with changes in the concentrations of other
redox-sensitive solutes in surface waters. Following drawdown, surface DO concentrations
decreased to a minimum of 41% saturation (3.5 mg/L), 43% lower than in 2021 (Figure 3b,
Figure 7). Loss of oxic epilimnetic water also resulted in increased anoxic extent as a proportion
of the water column in 2022 (Figure 3b). Comparing between years, total Fe concentrations
reached a peak 54% higher (by 0.34 µg/L) and 29 days earlier than in 2021, and soluble Fe
concentrations reached a peak 144% higher (by 0.42 µg/L) and 49 days earlier than in 2021
(Figure 7). Percent changes in Mn concentrations from 2021 to 2022 were even more substantial
than those of Fe. Total Mn concentrations reached a peak 201% higher (by 0.07 µg/L) and 29
days earlier than in 2021, and soluble Mn concentrations reached a peak 266% higher (by 0.02
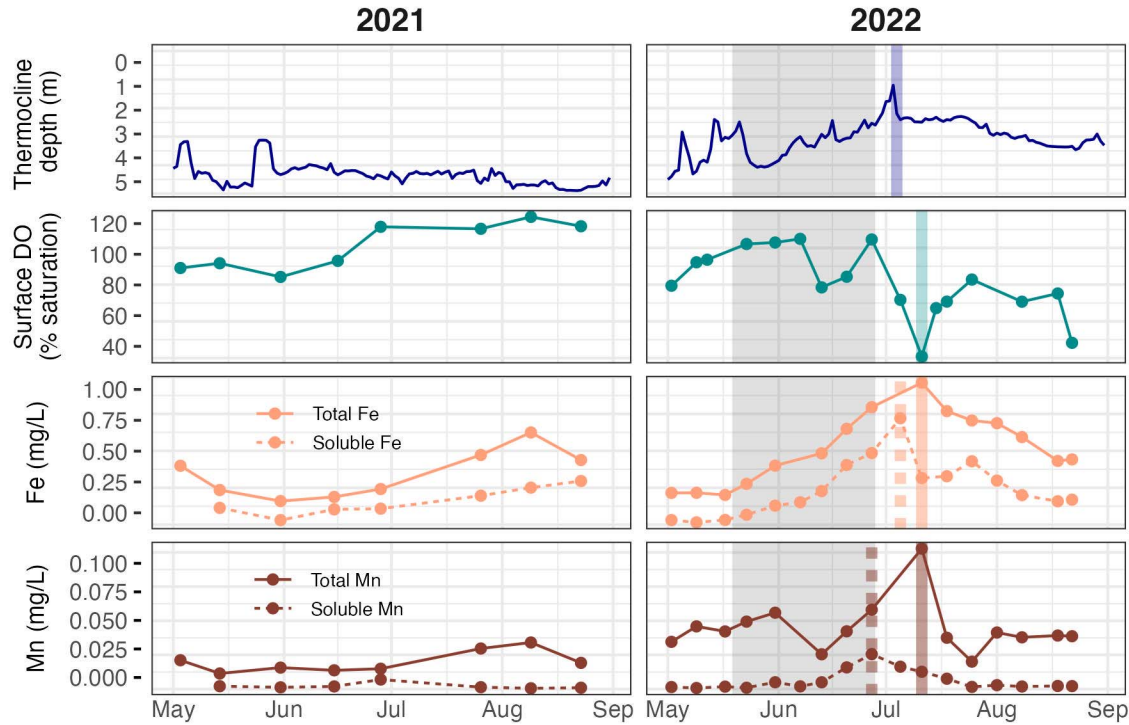µg/L) and 1 day earlier than in 2021 (Figure 7).

420

Figure 7: Time series of thermocline depth (m), surface dissolved oxygen (DO; % saturation), surface total Fe (mg/L) and surface total Mn (mg/L) at 0.1 m depth in Beaverdam Reservoir during summers 2021 and 2022. Gray shading indicates the drawdown period in 2022. Colored vertical lines indicate the observed maximum or minimum for each variable in 2022. Points represent discrete sampling visits, while the continuous line for thermocline depth was derived from high-frequency *in situ* sensors. Note reversed y-axis scale for thermocline depth, with 0 m corresponding to the reservoir surface.

4 Discussion

The month-long drawdown at Beaverdam Reservoir provided a unique opportunity to investigate the emergent responses that arise from multiple, interconnected ecosystem changes during drawdown. Coincident with drawdown, both stratification strength at the thermocline and surface SRP concentrations increased. These initial changes were followed by a substantial surface cyanobacterial bloom and sequential peaks in several biogeochemical variables associated with degradation of the bloom (e.g., DOC, dissolved CO_2). Our intensive monitoring during this management-driven drawdown provides an informative case study illustrating how changes in water level can have emergent effects on reservoir physics, chemistry, and biology in small, thermally-stratified reservoirs, which are underrepresented in the drawdown literature (Table S1).

4.1 Drawdown increased thermocline strength

Drawdown in Beaverdam Reservoir altered multiple aspects of reservoir physics (e.g., buoyancy frequency, Schmidt stability, epilimnion depth), with important implications for biogeochemical processing. Interestingly, our work highlighted the potential for drawdown to

16

444 increase the local strength of thermal stratification at the thermocline (i.e., maximum buoyancy
445 frequency; Figure 4). Maximum buoyancy frequency characterizes the likelihood of mixing
446 between surface and bottom layers in a stratified waterbody (e.g., Foley et al., 2012; Mackay et
447 al., 2014), which will affect depth profiles of water chemistry (Bush et al., 2017; MacIntyre et
448 al., 1999; Osborn, 1980) and phytoplankton (Cullen, 2015; Leach et al., 2018; Lofton et al.,
449 2020, 2022). Consequently, changes in thermocline strength have the potential to play an
450 important role in modulating the effect of drawdowns on reservoir chemistry and biology,
451 particularly during smaller drawdowns (i.e., those that do not result in destratification), like in
452 Beaverdam Reservoir. These smaller drawdowns are common worldwide as a result of changes
453 in climate and land use (Cooley et al., 2021; Kraemer et al., 2020; Ye et al., 2017; Zhao et al.,
454 2022), but are not well-characterized across existing literature (Table S1).

455   The observed increase in buoyancy frequency at the thermocline during drawdown could
456 have resulted from multiple mechanisms. Decreased residence time of water in the epilimnion
457 during drawdown (due to increased outflow rates from this layer) could reduce thermal exchange
458 between the epilimnion and hypolimnion, thereby steepening the temperature gradient at the
459 thermocline (Wang et al., 2012). Additionally, decreased epilimnetic volume could also increase
460 surface temperatures by allowing solar radiation and atmospheric heat to warm a smaller volume
461 of water (e.g., Pilla et al., 2018), and this higher temperature differential between surface and
462 bottom waters could increase maximum buoyancy frequency.

463   Across the drawdown literature, changes in local stratification strength at the thermocline
464 have received less attention than the susceptibility to full water column mixing during drawdown
465 (Table S1), despite the importance of thermocline strength for regulating reservoir chemistry and
466 biology (e.g., MacIntyre et al., 1999; Leach et al., 2018). Importantly, changes in buoyancy
467 frequency and Schmidt stability have different implications for biogeochemical processing.
468 Increases in buoyancy frequency limit mixing of solutes between the epilimnion and
469 hypolimnion, whereas decreases in Schmidt stability can (but do not always) lead to mixing
470 events that homogenize solutes throughout the water column (Bush et al., 2017; MacIntyre et al.,
471 1999; Osborn, 1980; Wetzel, 2001). Decreased water depth inherently reduces the amount of
472 energy required to mix the full water column, thereby resulting in decreased Schmidt stability,
473 documented here and elsewhere (see Table S1). However, in contrast to many previous
474 drawdown studies (summarized in Table S1), drawdown in Beaverdam Reservoir did not result
475 in full water column mixing or substantial hypolimnion deepening, making the decline in
476 Schmidt stability less relevant for biogeochemical cycling in the reservoir than the increase in
477 buoyancy frequency at the thermocline. Consequently, our work highlights the importance of
478 calculating multiple metrics of thermal stratification to understand the complex effects of
479 drawdown on reservoir physical processes.

480   4.1.1 Surface nutrient and metal concentrations increased, despite increased thermocline
481   strength

482   Although drawdown increased maximum buoyancy frequency, surface SRP
483 concentrations increased during drawdown, likely contributing to a substantial surface
484 phytoplankton bloom shortly thereafter (Figure 5). We also observed peaks of total and soluble
485 Fe and Mn in surface waters, which occurred several weeks after the increase in SRP and
486 coincided with the minimum surface DO (41% saturation) observed during this period (Figure
487 7). These effects are somewhat counterintuitive, as higher maximum buoyancy frequency would

488 be expected to decrease solute flux rates across the thermocline, thus resulting in lower solute
489 concentrations in the epilimnion (Bush et al., 2017). Our results suggest that shallowing of the
490 epilimnion may have concentrated nutrients in a smaller epilimnetic layer (Chapra & Reckhow,
491 1983; Snodgrass, 1977). This effect was likely exacerbated by wave action on newly exposed
492 sediments during drawdown, contributing to inputs of nutrients and metals from littoral areas
493 (Furey et al., 2004), as evident from increased turbidity during drawdown (Figure 6). Because
494 soluble Fe and Mn concentrations peaked earlier than total Fe and Mn concentrations (Figure 7),
495 it seems likely that these metals were entrained from the anoxic hypolimnion in their reduced
496 (soluble) state, before being oxidized in the epilimnion (Davison, 1993; Krueger et al., 2020;
497 Munger et al., 2019). In contrast, the earlier peak in SRP is more likely to have resulted from
498 littoral sediment inputs at the start of drawdown, though we note that direct attribution of either
499 of these mechanisms requires additional fine-scale measurements and/or mechanistic modeling
500 in future studies. Importantly, our results highlight that increases in surface nutrients during
501 drawdown, which are often documented in drawdowns that exhibit decreases in thermal stability
502 (Baldwin et al., 2008; Geraldes & Boavida, 2005; Naselli-Flores, 2003), can occur even when
503 the local strength of stratification at the thermocline increases.

504 4.2 Phytoplankton biomass and distribution were altered by nutrient and light dynamics

505 Drawdown in Beaverdam Reservoir resulted in simultaneous decreases in euphotic depth
506 (Figure 6) and increases in nutrient availability (Figure 5). Consequently, the net effect of
507 drawdown on phytoplankton biomass was challenging to predict *a priori*, as decreased light can
508 decrease phytoplankton growth, while increased nutrient availability can increase phytoplankton
509 growth. Altogether, we observed a substantial *increase* in surface phytoplankton biomass during
510 the drawdown, with a peak in phytoplankton biomass occurring approximately seven days after a
511 peak in SRP (Figure 5). Consequently, our work demonstrates that the nutrient increases
512 associated with drawdown can offset decreased light availability to result in an emergent
513 increase in phytoplankton biomass, at least in some cases. Additional studies are needed to test
514 the robustness of this response to drawdown in other reservoirs.

515 The vertical distribution of phytoplankton in the water column during the drawdown
516 differed from the distribution exhibited in the previous year, potentially in response to the
517 decreased light availability, shallowing of the thermocline, and increased surface nutrient
518 concentrations that occurred during drawdown. Notably, the decrease in C_{max} depth observed in
519 this study (Figure 6) was correlated with the euphotic zone depth becoming shallower during
520 drawdown (Figure S4). In previous summers, Beaverdam Reservoir has experienced
521 cyanobacterial blooms in the hypolimnion at depths with ≤1% of surface light, resulting in C_{max}
522 depths deeper than 7 m (Hamre et al., 2018). The bloom that occurred after the 2022 drawdown
523 was much closer to the surface than previous years, with maximum phytoplankton
524 concentrations occurring at C_{max} depths of ≤3 m (Figure 6). Interestingly, due to the altered light
525 environment (i.e., shallower euphotic zone depth) in the reservoir during drawdown, C_{max} depth
526 was associated with approximately the same light availability in 2022 as in previous years (~1%
527 of surface light), though at much shallower depths (Figures 6, S4). Our results support previous
528 work in a nearby reservoir that observed the reciprocal effect, in which thermocline deepening
529 led to a deepening of C_{max} depth (Lofton et al., 2022). Ultimately, these results highlight the
530 substantial plasticity of phytoplankton to adapt to changing physical conditions, optimizing their
531 location at the depth that best matches their nutrient and light requirements.

532   We observed that the peak width of phytoplankton biomass was approximately 2 m
533   thinner during drawdown than during the same time period in the previous year (Figure 6).
534   Declines in peak width could result from a number of factors, as phytoplankton exhibit higher
535   growth rates in layers of the water column with optimal temperature, light, and nutrient
536   conditions (Durham & Stocker, 2012; Moll et al., 1984). The steeper temperature gradient at the
537   thermocline during drawdown may have created a narrow range of depths where conditions were
538   optimal for growth, leading to aggregation of phytoplankton in a thinner layer. Likewise,
539   shallower euphotic zone depth and thermocline depth could have decreased suitable thermal and
540   light habitat (Hamilton et al., 2010; Leach et al., 2018; Varela et al., 1994). Ultimately, it is
541   likely that multiple factors collectively contributed to the development of thinner peak width of
542   phytoplankton biomass during drawdown. Altered spatial distribution of phytoplankton (i.e.,
543   decreased peak width) could potentially lead to heterogeneity in phytoplankton-driven
544   biogeochemical processing across the entire water column (e.g., Heini et al., 2014; Levine &
545   Lewis Jr., 1985) or affect zooplankton grazing dynamics (Moeller et al., 2019; Pilati &
546   Wurtsbaugh, 2003; Wang et al., 2020). In addition, concentration of phytoplankton in a narrower
547   layer of the water column could have potential water quality implications if these aggregations
548   occur at a depth from which water is withdrawn for drinking water treatment.

549   4.3.1 The phytoplankton bloom was associated with cascading effects on carbon and
550   nutrient cycling

551   The surface cyanobacterial bloom observed in 2022 was temporally associated with
552   marked changes in the dynamics of multiple biogeochemical variables (Figure 5). TN and TP
553   increased concurrently with phytoplankton, likely reflecting continuing nutrient inputs and
554   incorporation of N and P into phytoplankton biomass (Li et al., 2012). The subsequent peak in
555   DOC likely resulted from both leaching from live phytoplankton during the bloom and
556   decomposition of senescing phytoplankton after the bloom collapsed (Bartosiewicz et al., 2021;
557   Søndergaard et al., 2000). Dissolved CO_2 concentrations remained very low while phytoplankton
558   and DOC were at their highest—likely due to fixation into phytoplankton biomass—but peaked
559   6 days after the peak in DOC, when respiration rates likely surpassed fixation rates. Finally, the
560   peak in NH_4^+ three weeks after peak bloom conditions likely reflected ammonification from
561   decomposing organic matter (Gardner et al., 2017; Tezuka, 1986). In sum, the drawdown-
562   associated cyanobacterial bloom was associated with multiple changes in water chemistry,
563   substantially affecting coupled C, N, and P cycles in the reservoir.

564   Our results follow the findings of other studies with respect to the effects of
565   phytoplankton blooms on reservoir physics and biogeochemistry. Similar to our observations that
566   DOC, dissolved CO_2, and NH_4^+ peaked shortly (8–21 days) after peak cyanobacterial biomass
567   occurred, other researchers have documented that phytoplankton cell degradation and subsequent
568   leaching can occur rapidly, on the scale of hours to days (Hansen et al., 1986). Previous studies
569   have also similarly found that bloom degradation is associated with increases in dissolved
570   organic matter and dissolved CO_2 (Bartosiewicz et al., 2021; Søndergaard et al., 2000; Zhang et
571   al., 2022), as well as mineralization of both N (Gardner et al., 2017; Tezuka, 1986) and P (Carey
572   et al., 2014; Hałemejko & Chrost, 1984). While we did not collect microbial community data,
573   degradation of phytoplankton blooms is also associated with substantial changes in microbial
574   community structure as microbes decompose senescing phytoplankton cells (Fukami et al., 1983;
575   Grossart & Simon, 1998). Finally, dense growth of phytoplankton cells in surface water during
576   blooms can lead to increased light attenuation and, while not quantified in this study, heat

577 absorption, both affecting the underwater light environment and potentially prolonging or
578 stabilizing thermal stratification (Mesman et al., 2021; Robarts & Zohary, 1984; Zhang et al.,
579 2022). In sum, our work highlights that phytoplankton blooms due to reservoir drawdowns are
580 likely to have cascading effects on multiple aspects of reservoir ecosystem functioning.

581   4.3 Decreases in surface DO caused by bloom degradation and epilimnetic water loss

582   Despite atmospheric exchange, surface DO concentrations decreased substantially
583 following drawdown, which can have important consequences for higher trophic levels in the
584 reservoir. The magnitude of decline in surface water DO observed in our study (41% saturation
585 at 0.1 m depth) is remarkable in comparison to other drawdowns (Table S1). This decrease was
586 likely mediated in part by high oxygen demand due to decomposition of the decaying
587 phytoplankton bloom in surface water and oxidation of reduced solutes within the epilimnion
588 (see Section 4.1.1). Additionally, loss of epilimnetic water volume during drawdown decreased
589 the total epilimnetic oxygen mass amidst this high oxygen demand. Consequently, we anticipate
590 that low DO saturation may be particularly pronounced during the 2022 drawdown in
591 Beaverdam Reservoir (i.e., compared to other drawdowns) due to the synergistic effects of
592 bloom degradation and epilimnetic water loss (Figures 3, 5, 7). While zooplankton and fish
593 dynamics were not monitored in this study, the depth at which DO dropped below 3 mg/L (a
594 threshold below which many fish and zooplankton taxa cannot survive; e.g., Missaghi et al.,
595 2017; Stefan et al., 2001) was 3 m shallower in the drawdown year than the non-drawdown year,
596 and the temperature at which DO crossed this threshold was 7.5 ºC higher in 2022 than 2021
597 (Figure S5). Combined, these factors could force fish and zooplankton to congregate within a
598 shallower surface layer (McLaren et al., 2023), increase habitat overlap between zooplankton
599 and predatory fish (Dillon et al., 2021), and/or potentially eliminate habitat for coldwater fish
600 species (Missaghi et al., 2017; Stefan et al., 2001).

601   Interactions of physical, chemical, and biological variables make changes in surface DO
602 concentrations difficult to predict *a priori* as an emergent response of drawdown. A synthesis of
603 the previous literature on drawdowns (Table S1) indicates that surface DO can sometimes
604 decrease (Benejam et al., 2008; Cott et al., 2008; DeBoer et al., 2016; Naselli-Flores, 2003;
605 Saber et al., 2020), increase (Sánchez-Carrillo et al., 2007; Yang et al., 2016), or exhibit no
606 change during drawdown (Baldwin et al., 2008; Brasil et al., 2016; Geraldes & Boavida, 2005;
607 Magbanua et al., 2015). In general, surface water DO declines are more frequently reported for
608 management or experimental drawdowns and less frequently reported for natural drawdowns,
609 potentially due to correlated increases in surface primary production during many natural
610 drawdowns (Table S1). Consequently, our investigation of the effects of a management
611 drawdown in Beaverdam Reservoir provides a useful case study highlighting the emergent
612 effects of simultaneous changes in reservoir physics and biology driving DO dynamics in surface
613 water.

614   4.4 Strengths and limitations of whole-ecosystem drawdown experiment

615   Our intensive monitoring before, during, and after the management-driven drawdown in
616 Beaverdam Reservoir allowed us to identify potential effects of water level change on reservoir
617 physics, chemistry, and biology. Importantly, the substantial changes we observed in water
618 quality were not associated with corresponding increases in air temperature or decreases in
619 precipitation, as is typical of drought-driven drawdowns (Table S1), helping us to isolate the

620 impacts of water level separate from these other drivers. Still, this analysis is limited to one
621 drawdown and one waterbody, limiting inference into how time of year, lake type (e.g., dimictic
622 vs. polymictic, oligotrophic vs. eutrophic), or legacy effects of previous drawdowns may have
623 altered the results observed here. Without detailed mechanistic modeling, we are unable to
624 conclusively identify the mechanisms responsible for the changes observed in this study. Still,
625 the magnitude of change observed during Beaverdam's drawdown relative to the previous non-
626 drawdown year (e.g., phytoplankton concentrations 147% higher, NH_4^+ concentrations 2273%
627 higher) and intuitive mechanistic connections between the variables of interest (e.g., a DOC
628 increase coincident with bloom senescence) provide support for substantial drawdown-driven
629 effects on reservoir physics, chemistry, and biology. Ultimately, our work contributes to an
630 emerging body of research on the effects of drawdowns (Table S1) and motivates additional
631 research to characterize these events across a broader range of environmental conditions.

632   4.5 Emergent effects of drawdown vary among reservoirs and drawdowns

633   Altogether, our study highlights how the emergent effects of drawdown are likely
634 influenced by characteristics of an individual waterbody. At Beaverdam Reservoir, drawdown
635 was insufficient to allow light penetration to hypolimnetic sediment, likely due to the depth and
636 turbidity of the reservoir. However, if sufficient amounts of light did reach the sediments, we
637 may have observed warmed hypolimnetic water and increased benthic algae and/or macrophyte
638 growth, with consequent increases in whole-ecosystem DO, rather than the observed decrease
639 (Figure 1a). As a eutrophic reservoir, Beaverdam Reservoir already had high phytoplankton
640 biomass and hypolimnetic nutrient concentrations, which likely contributed to the observed
641 phytoplankton bloom that occurred during drawdown (Figure 1b). Similarly, presence of an
642 anoxic hypolimnion likely played a role in increasing nutrient fluxes to surface water and
643 decreasing surface DO concentrations following drawdown (Figure 2c). Altogether, our findings
644 and the results of previous research (Table S1) suggest that the volume of water lost during
645 drawdown, waterbody depth, clarity, outflow depth, and trophic state are likely all critical factors
646 for predicting the emergent effects of drawdown.

647   Our results provide a useful complement to previous research by demonstrating how loss
648 of epilimnetic water has the potential to substantially worsen, rather than improve, water quality
649 in some reservoirs. Previous management-driven drawdowns have often improved water quality,
650 as indicated by decreased phytoplankton biomass (Ejankowski & Solis, 2015; Matsuzaki et al.,
651 2023; Table S1), likely because these management interventions have removed hypolimnetic
652 water, increased light penetration to sediments, or destratified the waterbody. Removal of
653 hypolimnetic water releases nutrients from the ecosystem, and increased light penetration and
654 destratification can increase DO concentrations in bottom waters, thereby reducing internal
655 nutrient loads (e.g., Matsuzaki et al., 2023; Nürnberg, 2020). Conversely, removal of epilimnetic
656 water at Beaverdam Reservoir increased the surface concentrations of nutrients, contributing to
657 increased phytoplankton growth. As such, our results at Beaverdam Reservoir align more closely
658 with the effects of seasonal or drought-induced drawdowns than management-driven or
659 experimental drawdowns across the published literature. Seasonal and drought-induced
660 drawdowns have often resulted in increased phytoplankton biomass and worsening water quality,
661 though these effects have been difficult to disentangle from correlated seasonal changes in
662 temperature and hydrology (Table S1). Importantly, as climate change and water management
663 continue to increase the frequency and intensity of all types of drawdowns across lakes and

664 reservoirs worldwide, our results highlight the importance of characterizing how drawdown can
665 alter complex in-lake processes, thus affecting water quality.

666 **Acknowledgments**

678 **Open Research**

679   All data analyzed for this study are published in the Environmental Data Initiative
680 repository (Carey et al., 2022b, 2023a, 2023b, 2023c, 2023d, 2023e; Carey & Breef-Pilz, 2023;
681 Schreiber et al., 2023). Analysis code to reproduce the results in this manuscript is available in a
682 Zenodo repository (Lewis et al., 2023).

683 **References**

684 Alldredge, A., Cowles, T., Macintyre, S., Rines, J., Donaghay, P., Greenlaw, C., et al. (2002).
685   Occurrence and mechanics of formation of a dramatic thin layer of marine snow in a
686   shallow Pacific fjord. *Marine Ecology-Progress Series*, *233*, 1–12.
687   https://doi.org/10.3354/meps233001

688 Amani, M., von Schiller, D., Suárez, I., Atristain, M., Elosegi, A., Marcé, R., et al. (2022). The
689   drawdown phase of dam decommissioning is a hot moment of gaseous carbon emissions
690   from a temperate reservoir. *Inland Waters*, *12*(4), 451–462.
691   https://doi.org/10.1080/20442041.2022.2096977

692 Baldwin, D. S., Gigney, H., Wilson, J. S., Watson, G., & Boulding, A. N. (2008). Drivers of
693   water quality in a large water storage reservoir during a period of extreme drawdown.
694   *Water Research*, *42*(19), 4711–4724. https://doi.org/10.1016/j.watres.2008.08.020

695 Barbiero, R. P., James, W. F., & Barko, J. W. (1997). The effects of a change in withdrawal
696   operations on phytoplankton and nutrient dynamics in eau galle reservoir, Wisconsin
697   (USA). *Internationale Revue Der Gesamten Hydrobiologie Und Hydrographie*, *82*(4),
698   531–543. https://doi.org/10.1002/iroh.19970820410

699 Barley, S. C., & Meeuwig, J. J. (2017). The Power and the Pitfalls of Large-scale, Unreplicated
700   Natural Experiments. *Ecosystems*, *20*(2), 331–339. https://doi.org/10.1007/s10021-016-
701   0028-5

Bartosiewicz, M., Maranger, R., Przytulska, A., & Laurion, I. (2021). Effects of phytoplankton blooms on fluxes and emissions of greenhouse gases in a eutrophic lake. *Water Research*, *196*, 116985. https://doi.org/10.1016/j.watres.2021.116985

Beaulieu, J. J., Balz, D. A., Birchfield, M. K., Harrison, J. A., Nietch, C. T., Platz, M. C., et al. (2018). Effects of an Experimental Water-level Drawdown on Methane Emissions from a Eutrophic Reservoir. *Ecosystems*, *21*(4), 657–674. https://doi.org/10.1007/s10021-017-0176-2

Benejam, L., Benito, J., Ordóñez, J., Armengol, J., & García-Berthou, E. (2008). Short-term Effects of a Partial Drawdown on Fish Condition in a Eutrophic Reservoir. *Water, Air, and Soil Pollution*, *190*(1), 3–11. https://doi.org/10.1007/s11270-007-9574-y

Beutler, M., Wiltshire, K. H., Meyer, B., Moldaenke, C., Lüring, C., Meyerhöfer, M., et al. (2002). A fluorometric method for the differentiation of algal populations in vivo and in situ. *Photosynthesis Research*, *72*(1), 39–53. https://doi.org/10.1023/A:1016026607048

Brasil, J., Attayde, J. L., Vasconcelos, F. R., Dantas, D. D. F., & Huszar, V. L. M. (2016). Drought-induced water-level reduction favors cyanobacteria blooms in tropical shallow lakes. *Hydrobiologia*, *770*(1), 145–164. https://doi.org/10.1007/s10750-015-2578-5

Brenton, R. W., & Arnett, T. L. (1993). *Methods of analysis by the U.S. Geological Survey National Water Quality Laboratory-Determination of dissolved organic carbon by UV-promoted persulfate oxidation and infrared spectrometry* (USGS Numbered Series No. 92–480). U.S. Geological Survey. https://doi.org/10.3133/ofr92480

Bush, T., Diao, M., Allen, R. J., Sinnige, R., Muyzer, G., & Huisman, J. (2017). Oxic-anoxic regime shifts mediated by feedbacks between biogeochemical processes and microbial community dynamics. *Nature Communications*, *8*, 789. https://doi.org/10.1038/s41467-017-00912-x

Butcher, J. B., Nover, D., Johnson, T. E., & Clark, C. M. (2015). Sensitivity of lake thermal and mixing dynamics to climate change. *Climatic Change*, *129*(1), 295–305. https://doi.org/10.1007/s10584-015-1326-1

Carey, C. C., & Breef-Pilz, A. (2023). Time series of high-frequency meteorological data at Falling Creek Reservoir, Virginia, USA 2015-2022 [Data set]. Environmental Data Initiative. https://doi.org/10.6073/PASTA/F3F97C7FDD287C29084BF52FC759A801

Carey, C. C., Cottingham, K. L., Weathers, K. C., Brentrup, J. A., Ruppertsberger, N. M., Ewing, H. A., & Hairston, N. G., Jr. (2014). Experimental blooms of the cyanobacterium Gloeotrichia echinulata increase phytoplankton biomass, richness and diversity in an oligotrophic lake. *Journal of Plankton Research*, *36*(2), 364–377. https://doi.org/10.1093/plankt/fbt105

Carey, C. C., Hanson, P. C., Thomas, R. Q., Gerling, A. B., Hounshell, A. G., Lewis, A. S. L., et al. (2022a). Anoxia decreases the magnitude of the carbon, nitrogen, and phosphorus sink in freshwaters. *Global Change Biology*, *28*(16), 4861–4881. https://doi.org/10.1111/gcb.16228

Carey, C. C., Lewis, A. S. L., Howard, D. W., Woelmer, W. M., Gantzer, P. A., Bierlein, K. A., et al. (2022b). Bathymetry and watershed area for Falling Creek Reservoir, Beaverdam

Reservoir, and Carvins Cove Reservoir [Data set]. Environmental Data Initiative. https://doi.org/10.6073/PASTA/352735344150F7E77D2BC18B69A22412

Carey, C. C., Breef-Pilz, A., Wander, H. L., Geisler, B., & Haynie, G. (2023a). Secchi depth data and discrete depth profiles of water temperature, dissolved oxygen, conductivity, specific conductance, photosynthetic active radiation, redox potential, and pH for Beaverdam Reservoir, Carvins Cove Reservoir, Falling Creek Reservoir, Gatewood Reservoir, and Spring Hollow Reservoir in southwestern Virginia, USA 2013-2022 [Data set]. Environmental Data Initiative. https://doi.org/10.6073/PASTA/EB17510D09E66EF79D7D54A18CA91D61

Carey, C. C., Lewis, A. S. L., Niederlehner, B. R., Breef-Pilz, A., Das, A., Geisler, B., & Haynie, G. (2023b). Time series of dissolved methane and carbon dioxide concentrations for Falling Creek Reservoir and Beaverdam Reservoir in southwestern Virginia, USA during 2015-2022 [Data set]. Environmental Data Initiative. https://doi.org/10.6073/PASTA/98E09AB2610FE9C348A8F09F0AA1DE53

Carey, C. C., Breef-Pilz, A., Bookout, B. J., McClure, R. P., & Wynne, J. H. (2023c). Time series of high-frequency sensor data measuring water temperature, dissolved oxygen, conductivity, specific conductance, total dissolved solids, chlorophyll a, phycocyanin, fluorescent dissolved organic matter, and turbidity at discrete depths in Beaverdam Reservoir, Virginia, USA in 2016-2022 [Data set]. Environmental Data Initiative. https://doi.org/10.6073/PASTA/4182DE376FDE52E15D493FDD9F26D0C7

Carey, C. C., Breef-Pilz, A., & Lofton, M. E. (2023d). Time-series of high-frequency profiles of fluorescence-based phytoplankton spectral groups in Beaverdam Reservoir, Carvins Cove Reservoir, Falling Creek Reservoir, Gatewood Reservoir, and Spring Hollow Reservoir in southwestern Virginia, USA 2014-2022 [Data set]. Environmental Data Initiative. https://doi.org/10.6073/PASTA/E12D218E1634674966BD03CFC3C7296E

Carey, C. C., Wander, H. L., Howard, D. W., Breef-Pilz, A., & Niederlehner, B. R. (2023e). Water chemistry time series for Beaverdam Reservoir, Carvins Cove Reservoir, Falling Creek Reservoir, Gatewood Reservoir, and Spring Hollow Reservoir in southwestern Virginia, USA 2013-2022 [Data set]. Environmental Data Initiative. https://doi.org/10.6073/PASTA/457120A9DE886A1470C22A01D808AB2D

Catherine, A., Escoffier, N., Belhocine, A., Nasri, A. B., Hamlaoui, S., Yepremian, C., et al. (2012). On the use of the FluoroProbe (R), a phytoplankton quantification method based on fluorescence excitation spectra for large-scale surveys of lakes and reservoirs. *Water Research*, *46*, 1771–84. https://doi.org/10.1016/j.watres.2011.12.056

Chapra, K. H., & Reckhow, S. C. (1983). *Engineering Approaches for Lake Management* (First Edition, Vol. 2). Boston: Butterworth.

Cooley, S. W., Ryan, J. C., & Smith, L. C. (2021). Human alteration of global surface water storage variability. *Nature*, *591*(7848), 78–81. https://doi.org/10.1038/s41586-021-03262-3

Coops, H., Beklioglu, M., & Crisman, T. L. (2003). The role of water-level fluctuations in shallow lake ecosystems – workshop conclusions. *Hydrobiologia*, *506*(1), 23–27. https://doi.org/10.1023/B:HYDR.0000008595.14393.77

785 Cott, P. A., Sibley, P. K., Gordon, A. M., Bodaly, R. A. (Drew), Mills, K. H., Somers, W. M., &
786   Fillatre, G. A. (2008). Effects of Water Withdrawal From Ice-Covered Lakes on Oxygen,
787   Temperature, and Fish1. *JAWRA Journal of the American Water Resources Association*,
788   *44*(2), 328–342. https://doi.org/10.1111/j.1752-1688.2007.00165.x

789 Cullen, J. J. (2015). Subsurface Chlorophyll Maximum Layers: Enduring Enigma or Mystery
790   Solved? *Annual Review of Marine Science*, *7*(1), 207–239.
791   https://doi.org/10.1146/annurev-marine-010213-135111

792 Davison, W. (1993). Iron and manganese in lakes. *Earth-Science Reviews*, *34*(2), 119–163.
793   https://doi.org/10.1016/0012-8252(93)90029-7

794 DeBoer, J. A., Webber, C. M., Dixon, T. A., & Pope, K. L. (2016). The influence of a severe
795   reservoir drawdown on springtime zooplankton and larval fish assemblages in Red
796   Willow Reservoir, Nebraska. *Journal of Freshwater Ecology*, *31*(1), 131–146.
797   https://doi.org/10.1080/02705060.2015.1055312

798 Deemer, B. R., & Harrison, J. A. (2019). Summer Redox Dynamics in a Eutrophic Reservoir and
799   Sensitivity to a Summer's End Drawdown Event. *Ecosystems*, *22*(7), 1618–1632.
800   https://doi.org/10.1007/s10021-019-00362-0

801 Dillon, R. A., Conroy, J. D., Lang, K. J., Pangle, K. L., & Ludsin, S. A. (2021). Bottom hypoxia
802   alters the spatial distribution of pelagic intermediate consumers and their prey. *Canadian*
803   *Journal of Fisheries and Aquatic Sciences*, *78*(5), 522–538. https://doi.org/10.1139/cjfas-
804   2020-0001

805 Doubek, J. P., Campbell, K. L., Doubek, K. M., Hamre, K. D., Lofton, M. E., McClure, R. P., et
806   al. (2018). The effects of hypolimnetic anoxia on the diel vertical migration of freshwater
807   crustacean zooplankton. *Ecosphere*, *9*(7), e02332. https://doi.org/10.1002/ecs2.2332

808 Downing, J. A., Prairie, Y. T., Cole, J. J., Duarte, C. M., Tranvik, L. J., Striegl, R. G., et al.
809   (2006). The global abundance and size distribution of lakes, ponds, and impoundments.
810   *Limnology and Oceanography*, *51*(5), 2388–2397.
811   https://doi.org/10.4319/lo.2006.51.5.2388

812 Durham, W. M., & Stocker, R. (2012). Thin Phytoplankton Layers: Characteristics, Mechanisms,
813   and Consequences. *Annual Review of Marine Science*, *4*(1), 177–207.
814   https://doi.org/10.1146/annurev-marine-120710-100957

815 Ejankowski, W., & Solis, M. (2015). Response of hornwort (Ceratophyllum Demersum L.) to
816   water level drawdown in a turbid water reservoir. *Applied Ecology and Environmental*
817   *Research*, *13*, 219–228. https://doi.org/10.15666/aeer/1301_219228

818 Fergus, C. E., Brooks, J. R., Kaufmann, P. R., Pollard, A. I., Mitchell, R., Geldhof, G. J., et al.
819   (2022). Natural and anthropogenic controls on lake water-level decline and evaporation-
820   to-inflow ratio in the conterminous United States. *Limnology and Oceanography*, *67*(7),
821   1484–1501. https://doi.org/10.1002/lno.12097

822 Foley, B., Jones, I. D., Maberly, S. C., & Rippey, B. (2012). Long-term changes in oxygen
823   depletion in a small temperate lake: effects of climate change and eutrophication.
824   *Freshwater Biology*, *57*(2), 278–289. https://doi.org/10.1111/j.1365-2427.2011.02662.x

825 Fukami, K., Simidu, U., & Taga, N. (1983). Change in a bacterial population during the process
826   of degradation of a phytoplankton bloom in a brackish lake. *Marine Biology*, *76*(3), 253–
827   255. https://doi.org/10.1007/BF00393025

828 Furey, P. C., Nordin, R. N., & Mazumder, A. (2004). Water Level Drawdown Affects Physical
829   and Biogeochemical Properties of Littoral Sediments of a Reservoir and a Natural Lake.
830   *Lake and Reservoir Management*, *20*(4), 280–295.
831   https://doi.org/10.1080/07438140409354158

832 Gardner, W. S., Newell, S. E., McCarthy, M. J., Hoffman, D. K., Lu, K., Lavrentyev, P. J., et al.
833   (2017). Community Biological Ammonium Demand: A Conceptual Model for
834   Cyanobacteria Blooms in Eutrophic Lakes. *Environmental Science & Technology*,
835   *51*(14), 7785–7793. https://doi.org/10.1021/acs.est.6b06296

836 Geraldes, A. M., & Boavida, M.-J. (2005). Seasonal water level fluctuations: Implications for
837   reservoir limnology and management. *Lakes & Reservoirs: Science, Policy and*
838   *Management for Sustainable Use*, *10*(1), 59–69. https://doi.org/10.1111/j.1440-
839   1770.2005.00257.x

840 Grossart, H.-P., & Simon, M. (1998). Bacterial colonization and microbial decomposition of
841   limnetic organic aggregates (lake snow). *Aquatic Microbial Ecology*, *15*(2), 127–140.
842   https://doi.org/10.3354/ame015127

843 Hałemejko, G. Z., & Chrost, R. (1984). The role of phosphatase in phosphorus mineralization
844   during decomposition of lake phytoplankton blooms. *Archiv Fur Hydrobiologie*, *101*,
845   489–502.

846 Hamilton, D. P., O'Brien, K. R., Burford, M. A., Brookes, J. D., & McBride, C. G. (2010).
847   Vertical distributions of chlorophyll in deep, warm monomictic lakes. *Aquatic Sciences*,
848   *72*(3), 295–307. https://doi.org/10.1007/s00027-010-0131-1

849 Hamre, K. D., Lofton, M. E., McClure, R. P., Munger, Z. W., Doubek, J. P., Gerling, A. B., et al.
850   (2018). In situ fluorometry reveals a persistent, perennial hypolimnetic cyanobacterial
851   bloom in a seasonally anoxic reservoir. *Freshwater Science*, *37*(3), 483–495.
852   https://doi.org/10.1086/699327

853 Hannoun, D., & Tietjen, T. (2023). Lake management under severe drought: Lake Mead,
854   Nevada/Arizona. *JAWRA Journal of the American Water Resources Association*, *59*(2),
855   416–428. https://doi.org/10.1111/1752-1688.13090

856 Hansen, L., Krog, G. F., & Søndergaard, M. (1986). Decomposition of Lake Phytoplankton. 1.
857   Dynamics of Short-Term Decomposition. *Oikos*, *46*(1), 37–44.
858   https://doi.org/10.2307/3565377

859 Harrison, J. A., Deemer, B. R., Birchfield, M. K., & O'Malley, M. T. (2017). Reservoir Water-
860   Level Drawdowns Accelerate and Amplify Methane Emission. *Environmental Science &*
861   *Technology*, *51*(3), 1267–1277. https://doi.org/10.1021/acs.est.6b03185

862 Heini, A., Puustinen, I., Tikka, M., Jokiniemi, A., Leppäranta, M., & Arvola, L. (2014). Strong
863   dependence between phytoplankton and water chemistry in a large temperate lake: spatial
864   and temporal perspective. *Hydrobiologia*, *731*(1), 139–150.
865   https://doi.org/10.1007/s10750-013-1777-1

Idso, S. B. (1973). On the concept of lake stability1. *Limnology and Oceanography*, *18*(4), 681–683. https://doi.org/10.4319/lo.1973.18.4.0681

Jiang, T., Wang, D., Wei, S., Yan, J., Liang, J., Chen, X., et al. (2018). Influences of the alternation of wet-dry periods on the variability of chromophoric dissolved organic matter in the water level fluctuation zone of the Three Gorges Reservoir area, China. *Science of The Total Environment*, *636*, 249–259. https://doi.org/10.1016/j.scitotenv.2018.04.262

Jones, I., George, G., & Reynolds, C. (2005). Quantifying effects of phytoplankton on the heat budgets of two large limnetic enclosures. *Freshwater Biology*, *50*, 1239–1247. https://doi.org/10.1111/j.1365-2427.2005.01397.x

Kasprzak, P., Shatwell, T., Gessner, M. O., Gonsiorczyk, T., Kirillin, G., Selmeczy, G., et al. (2017). Extreme Weather Event Triggers Cascade Towards Extreme Turbidity in a Clear-water Lake. *Ecosystems*, *20*(8), 1407–1420. https://doi.org/10.1007/s10021-017-0121-4

Keller, P. S., Marcé, R., Obrador, B., & Koschorreck, M. (2021). Global carbon budget of reservoirs is overturned by the quantification of drawdown areas. *Nature Geoscience*, *14*(6), 402–408. https://doi.org/10.1038/s41561-021-00734-z

Klotz, R. L., & Linn, S. A. (2001). Influence of Factors Associated with Water Level Drawdown on Phosphorus Release from Sediments. *Lake and Reservoir Management*, *17*(1), 48–54. https://doi.org/10.1080/07438140109353972

Kosten, S., van den Berg, S., Mendonça, R., Paranaíba, J. R., Roland, F., Sobek, S., et al. (2018). Extreme drought boosts CO_2 and CH_4 emissions from reservoir drawdown areas. *Inland Waters*, *8*(3), 329–340. https://doi.org/10.1080/20442041.2018.1483126

Kraemer, B. M., Anneville, O., Chandra, S., Dix, M., Kuusisto, E., Livingstone, D. M., et al. (2015). Morphometry and average temperature affect lake stratification responses to climate change. *Geophysical Research Letters*, *42*(12), 4981–4988. https://doi.org/10.1002/2015GL064097

Kraemer, B. M., Seimon, A., Adrian, R., & McIntyre, P. B. (2020). Worldwide lake level trends and responses to background climate variation. *Hydrology and Earth System Sciences*, *24*(5), 2593–2608. https://doi.org/10.5194/hess-24-2593-2020

Kring, S. A., Figary, S. E., Boyer, G. L., Watson, S. B., & Twiss, M. R. (2014). Rapid in situ measures of phytoplankton communities using the bbe FluoroProbe: evaluation of spectral calibration, instrument intercompatibility, and performance range. *Canadian Journal of Fisheries and Aquatic Sciences*, *71*(7), 1087–1095. https://doi.org/10.1139/cjfas-2013-0599

Krueger, K. M., Vavrus, C. E., Lofton, M. E., McClure, R. P., Gantzer, P., Carey, C. C., & Schreiber, M. E. (2020). Iron and manganese fluxes across the sediment-water interface in a drinking water reservoir. *Water Research*, *182*, 116003. https://doi.org/10.1016/j.watres.2020.116003

Kumagai, M., Nakano, S., Jiao, C., Hayakawa, K., Tsujimura, S., Nakajima, T., et al. (2000). Effect of cyanobacterial blooms on thermal stratification. *Limnology*, *1*(3), 191–195. https://doi.org/10.1007/s102010070006

907 Leach, T. H., Beisner, B. E., Carey, C. C., Pernica, P., Rose, K. C., Huot, Y., et al. (2018).
908　　　　Patterns and drivers of deep chlorophyll maxima structure in 100 lakes: The relative
909　　　　importance of light and thermal stratification. *Limnology and Oceanography*, *63*(2), 628–
910　　　　646. https://doi.org/10.1002/lno.10656

911 Levine, S. N., & Lewis Jr., W. M. (1985). The horizontal heterogeneity of nitrogen fixation in
912　　　　Lake Valencia, Venezuela1. *Limnology and Oceanography*, *30*(6), 1240–1245.
913　　　　https://doi.org/10.4319/lo.1985.30.6.1240

914 Lewis, A., Lofton, M., Breef-Pilz, A., & Olsson, F. (2023, September 9).
915　　　　abbylewis/BVR_Drawdown: Effects of a 2022 drawdown on water quality in Beaverdam
916　　　　Reservoir (Version v1.0.0). Zenodo. https://doi.org/10.5281/ZENODO.8330110

917 Lewis, D. M., Brereton, A., & Siddons, J. T. (2017). A large eddy simulation study of the
918　　　　formation of deep chlorophyll/biological maxima in un-stratified mixed layers: The roles
919　　　　of turbulent mixing and predation pressure. *Limnology and Oceanography*, *62*(5), 2277–
920　　　　2307. https://doi.org/10.1002/lno.10566

921 Li, Y., Waite, A. M., Gal, G., & Hipsey, M. R. (2012). Do phytoplankton nutrient ratios reflect
922　　　　patterns of water column nutrient ratios? A numerical stoichiometric analysis of Lake
923　　　　Kinneret. *Procedia Environmental Sciences*, *13*, 1630–1640.
924　　　　https://doi.org/10.1016/j.proenv.2012.01.156

925 Li, Y., Huang, T., Zhou, Z., Long, S., & Zhang, H. (2017). Effects of reservoir operation and
926　　　　climate change on thermal stratification of a canyon-shaped reservoir, in northwest
927　　　　China. *Water Supply*, *18*(2), 418–429. https://doi.org/10.2166/ws.2017.068

928 Liu, J., Deng, J., Chai, Y., Yang, Y., Zhu, B., & Li, S. (2019). Variation of the Water Level in
929　　　　the Yangtze River in Response to Natural and Anthropogenic Changes. *Water*, *11*(12),
930　　　　2594. https://doi.org/10.3390/w11122594

931 Lofton, M. E., Leach, T. H., Beisner, B. E., & Carey, C. C. (2020). Relative importance of top-
932　　　　down vs. bottom-up control of lake phytoplankton vertical distributions varies among
933　　　　fluorescence-based spectral groups. *Limnology and Oceanography*, *65*(10), 2485–2501.
934　　　　https://doi.org/10.1002/lno.11465

935 Lofton, M. E., Howard, D. W., McClure, R. P., Wander, H. L., Woelmer, W. M., Hounshell, A.
936　　　　G., et al. (2022). Experimental thermocline deepening alters vertical distribution and
937　　　　community structure of phytoplankton in a 4-year whole-reservoir manipulation.
938　　　　*Freshwater Biology*, *67*(11), 1903–1924. https://doi.org/10.1111/fwb.13983

939 Ma, J., Loiselle, S., Cao, Z., Qi, T., Shen, M., Luo, J., et al. (2023). Unbalanced impacts of
940　　　　nature and nurture factors on the phenology, area and intensity of algal blooms in global
941　　　　large lakes: MODIS observations. *Science of The Total Environment*, 163376.
942　　　　https://doi.org/10.1016/j.scitotenv.2023.163376

943 MacIntyre, S., Flynn, K. M., Jellison, R., & Romero, J. R. (1999). Boundary mixing and nutrient
944　　　　fluxes in Mono Lake, California. *Limnology and Oceanography*, *44*(3), 512–529.
945　　　　https://doi.org/10.4319/lo.1999.44.3.0512

946 Mackay, E. B., Folkard, A. M., & Jones, I. D. (2014). Interannual variations in atmospheric
947　　　　forcing determine trajectories of hypolimnetic soluble reactive phosphorus supply in a

948   eutrophic lake. *Freshwater Biology*, *59*(8), 1646–1658.
949   https://doi.org/10.1111/fwb.12371

950   Magbanua, F. S., Mendoza, N. Y. B., Uy, C. J. C., Matthaei, C. D., & Ong, P. S. (2015). Water
951   physicochemistry and benthic macroinvertebrate communities in a tropical reservoir: The
952   role of water level fluctuations and water depth. *Limnologica*, *55*, 13–20.
953   https://doi.org/10.1016/j.limno.2015.10.002

954   Magee, M. R., & Wu, C. H. (2017). Effects of changing climate on ice cover in three
955   morphometrically different lakes. *Hydrological Processes*, *31*(2), 308–323.
956   https://doi.org/10.1002/hyp.10996

957   Matsuzaki, S. S., Kohzu, A., Tsuchiya, K., Shinohara, R., Nakagawa, M., Fukumori, K., et al.
958   (2023). Water-level drawdowns can improve surface water quality and alleviate bottom
959   hypoxia in shallow, eutrophic water bodies. *Freshwater Biology*, *68*(2), 229–244.
960   https://doi.org/10.1111/fwb.14020

961   McClure, R. P., Hamre, K. D., Niederlehner, B. R., Munger, Z. W., Chen, S., Lofton, M. E., et
962   al. (2018). Metalimnetic oxygen minima alter the vertical profiles of carbon dioxide and
963   methane in a managed freshwater reservoir. *Science of The Total Environment*, *636*, 610–
964   620. https://doi.org/10.1016/j.scitotenv.2018.04.255

965   McClure, R. P., Lofton, M. E., Chen, S., Krueger, K. M., Little, J. C., & Carey, C. C. (2020). The
966   Magnitude and Drivers of Methane Ebullition and Diffusion Vary on a Longitudinal
967   Gradient in a Small Freshwater Reservoir. *Journal of Geophysical Research:*
968   *Biogeosciences*, *125*(3), e2019JG005205. https://doi.org/10.1029/2019JG005205

969   McLaren, J. S., Van Kirk, R. W., Mabaka, A. J., Brothers, S., & Budy, P. (2023). Drawdown,
970   Habitat, and Kokanee Populations in a Western U.S. Reservoir. *North American Journal*
971   *of Fisheries Management*, *43*(2), 339–351. https://doi.org/10.1002/nafm.10879

972   Mesman, J. P., Stelzer, J. A. A., Dakos, V., Goyette, S., Jones, I. D., Kasparian, J., et al. (2021).
973   The role of internal feedbacks in shifting deep lake mixing regimes under a warming
974   climate. *Freshwater Biology*, *66*(6), 1021–1035. https://doi.org/10.1111/fwb.13704

975   Missaghi, S., Hondzo, M., & Herb, W. (2017). Prediction of lake water temperature, dissolved
976   oxygen, and fish habitat under changing climate. *Climatic Change*, *141*.
977   https://doi.org/10.1007/s10584-017-1916-1

978   Moeller, H. V., Laufkötter, C., Sweeney, E. M., & Johnson, M. D. (2019). Light-dependent
979   grazing can drive formation and deepening of deep chlorophyll maxima. *Nature*
980   *Communications*, *10*(1), 1978. https://doi.org/10.1038/s41467-019-09591-2

981   Moll, R. A., Brache, M. Z., & Peterson, T. P. (1984). Phytoplankton dynamics within the
982   subsurface chlorophyll maximum of Lake Michigan 1. *Journal of Plankton Research*,
983   *6*(5), 751–766. https://doi.org/10.1093/plankt/6.5.751

984   Moreno-Ostos, E., Marcé, R., Ordóñez, J., Dolz, J., & Armengol, J. (2008). Hydraulic
985   Management Drives Heat Budgets and Temperature Trends in a Mediterranean
986   Reservoir. *International Review of Hydrobiology*, *93*(2), 131–147.
987   https://doi.org/10.1002/iroh.200710965

Munger, Z. W., Carey, C. C., Gerling, A. B., Doubek, J. P., Hamre, K. D., McClure, R. P., & Schreiber, M. E. (2019). Oxygenation and hydrologic controls on iron and manganese mass budgets in a drinking-water reservoir. *Lake and Reservoir Management*, *35*(3), 277–291. https://doi.org/10.1080/10402381.2018.1545811

Nakanishi, K., Yokomizo, H., Fukaya, K., Kadoya, T., Matsuzaki, S. S., Nishihiro, J., et al. (2022). Inferring causal impacts of extreme water-level drawdowns on lake water clarity using long-term monitoring data. *Science of The Total Environment*, *838*, 156088. https://doi.org/10.1016/j.scitotenv.2022.156088

Naselli-Flores, L. (2003). Man-made lakes in Mediterranean semi-arid climate: the strange case of Dr Deep Lake and Mr Shallow Lake. *Hydrobiologia*, *506*(1), 13–21. https://doi.org/10.1023/B:HYDR.0000008550.34409.06

Naselli-Flores, L., & Barone, R. (2005). Water-Level Fluctuations in Mediterranean Reservoirs: Setting a Dewatering Threshold as a Management Tool to Improve Water Quality. *Hydrobiologia*, *548*(1), 85–99. https://doi.org/10.1007/s10750-005-1149-6

Nürnberg, G. K. (2007). Lake responses to long-term hypolimnetic withdrawal treatments. *Lake and Reservoir Management*, *23*(4), 388–409. https://doi.org/10.1080/07438140709354026

Nürnberg, G. K. (2020). Hypolimnetic withdrawal as a lake restoration technique: determination of feasibility and continued benefits. *Hydrobiologia*, *847*(21), 4487–4501. https://doi.org/10.1007/s10750-019-04094-z

Odum, H. T. (1956). Primary Production in Flowing Waters1. *Limnology and Oceanography*, *1*(2), 102–117. https://doi.org/10.4319/lo.1956.1.2.0102

Osborn, T. R. (1980). Estimates of the Local Rate of Vertical Diffusion from Dissipation Measurements. *Journal of Physical Oceanography*, *10*(1), 83–89. https://doi.org/10.1175/1520-0485(1980)010<0083:EOTLRO>2.0.CO;2

Ouyang, W., Li, Z., Yang, J., Lu, L., & Guo, J. (2021). Spatio-Temporal Variations in Phytoplankton Communities in Sediment and Surface Water as Reservoir Drawdown—A Case Study of Pengxi River in Three Gorges Reservoir, China. *Water*, *13*(3), 340. https://doi.org/10.3390/w13030340

Perrin, C. J., Ashley, K. I., & Larkin, G. A. (2000). Effect of Drawdown on Ammonium and Iron Concentrations in a Coastal Mountain Reservoir. *Water Quality Research Journal*, *35*(2), 231–244. https://doi.org/10.2166/wqrj.2000.015

Pilati, A., & Wurtsbaugh, W. A. (2003). Importance of zooplankton for the persistence of a deep chlorophyll layer: A limnocorral experiment. *Limnology and Oceanography*, *48*(1), 249–260. https://doi.org/10.4319/lo.2003.48.1.0249

Pilla, R. M., Williamson, C. E., Zhang, J., Smyth, R. L., Lenters, J. D., Brentrup, J. A., et al. (2018). Browning-Related Decreases in Water Transparency Lead to Long-Term Increases in Surface Water Temperature and Thermal Stratification in Two Small Lakes. *Journal of Geophysical Research: Biogeosciences*, *123*(5), 1651–1665. https://doi.org/10.1029/2017JG004321

1028 Planas, D., & Paquet, S. (2016). Importance of climate change-physical forcing on the increase
1029   of cyanobacterial blooms in a small, stratified lake. *Journal of Limnology*, *75*(s1).
1030   https://doi.org/10.4081/jlimnol.2016.1371

1031 Read, J. S., Hamilton, D. P., Jones, I. D., Muraoka, K., Winslow, L. A., Kroiss, R., et al. (2011).
1032   Derivation of lake mixing and stratification indices from high-resolution lake buoy data.
1033   *Environmental Modelling & Software*, *26*(11), 1325–1336.
1034   https://doi.org/10.1016/j.envsoft.2011.05.006

1035 Rimmer, A., Gal, G., Opher, T., Lechinsky, Y., & Yacobi, Y. Z. (2011). Mechanisms of long-
1036   term variations in the thermal structure of a warm lake. *Limnology and Oceanography*,
1037   *56*(3), 974–988. https://doi.org/10.4319/lo.2011.56.3.0974

1038 Rinke, K., Huber, A. M. R., Kempke, S., Eder, M., Wolf, T., Probst, W. N., & Rothhaupta, K.-O.
1039   (2009). Lake-wide distributions of temperature, phytoplankton, zooplankton, and fish in
1040   the pelagic zone of a large lake. *Limnology and Oceanography*, *54*(4), 1306–1322.
1041   https://doi.org/10.4319/lo.2009.54.4.1306

1042 Robarts, R. D., & Zohary, T. (1984). Microcystis Aeruginosa and Underwater Light Attenuation
1043   in a Hypertrophic Lake (Hartbeespoort Dam, South Africa). *Journal of Ecology*, *72*(3),
1044   1001–1017. https://doi.org/10.2307/2259547

1045 Saber, A., James, D. E., & Hannoun, I. A. (2020). Effects of lake water level fluctuation due to
1046   drought and extreme winter precipitation on mixing and water quality of an alpine lake,
1047   Case Study: Lake Arrowhead, California. *Science of The Total Environment*, *714*,
1048   136762. https://doi.org/10.1016/j.scitotenv.2020.136762

1049 Sánchez-Carrillo, S., Alatorre, L. C., Sánchez-Andrés, R., & Garatuza-Payán, J. (2007).
1050   Eutrophication and Sedimentation Patterns in Complete Exploitation of Water Resources
1051   Scenarios: An Example from Northwestern Semi-arid Mexico. *Environmental
1052   Monitoring and Assessment*, *132*(1), 377–393. https://doi.org/10.1007/s10661-006-9541-
1053   x

1054 Schreiber, M. E., Ming, C. L., Hammond, N. W., Breef-Pilz, A., Geisler, B., & Haynie, G.
1055   (2023). Time series of total and soluble iron and manganese concentrations from Falling
1056   Creek Reservoir, Beaverdam Reservoir and Carvins Cove Reservoir in southwestern
1057   Virginia, USA from 2014 through 2022 [Data set]. Environmental Data Initiative.
1058   https://doi.org/10.6073/PASTA/9D901AE44871E018F475F42C58FB2004

1059 Snodgrass, W. J. (1977). Relationship of Vertical Transport Across the Thermocline to Oxygen
1060   and Phosphorus Regimes: Lake Ontario as a Prototype. In R. J. Gibbs & R. P. Shaw
1061   (Eds.), *Transport Processes in Lakes and Oceans* (pp. 179–202). Boston, MA: Springer
1062   US. https://doi.org/10.1007/978-1-4684-2760-8_9

1063 Søndergaard, M., Borch, N., & Riemann, B. (2000). Dynamics of biodegradable DOC produced
1064   by freshwater plankton communities. *Aquatic Microbial Ecology - AQUAT MICROB
1065   ECOL*, *23*, 73–83. https://doi.org/10.3354/ame023073

1066 Stefan, H., Fang, X., & Eaton, J. (2001). Simulated Fish Habitat Changes in North American
1067   Lakes in Response to Projected Climate Warming. *Transactions of the American
1068   Fisheries Society*, *130*, 459–477. https://doi.org/10.1577/1548-
1069   8659(2001)130<0459:SFHCIN>2.0.CO;2

1070 Tezuka, Y. (1986). Does the seston of Lake Biwa release dissolved inorganic nitrogen and
1071   phosphorus during aerobic decomposition?: Its implication for eutrophication. *Ecological*
1072   *Research*, *1*(3), 293–302. https://doi.org/10.1007/BF02348686

1073 U.S. Army Corps of Engineers. (2021). National Inventory of Dams [Data set]. Retrieved from
1074   https://nid.sec.usace.army.mil/

1075 Varela, R. A., Cruzado, A., & Tintoré, J. (1994). A simulation analysis of various biological and
1076   physical factors influencing the deep-chlorophyll maximum structure in oligotrophic
1077   areas. *Journal of Marine Systems*, *5*(2), 143–157. https://doi.org/10.1016/0924-
1078   7963(94)90028-0

1079 Wada, Y., Wisser, D., & Bierkens, M. F. P. (2014). Global modeling of withdrawal, allocation
1080   and consumptive use of surface water and groundwater resources. *Earth System*
1081   *Dynamics*, *5*(1), 15–40. https://doi.org/10.5194/esd-5-15-2014

1082 Wang, L., Shen, H., Wu, Z., Yu, Z., Li, Y., Su, H., et al. (2020). Warming affects crustacean
1083   grazing pressure on phytoplankton by altering the vertical distribution in a stratified lake.
1084   *Science of The Total Environment*, *734*, 139195.
1085   https://doi.org/10.1016/j.scitotenv.2020.139195

1086 Wang, S., Qian, X., Han, B.-P., Luo, L.-C., & Hamilton, D. P. (2012). Effects of local climate
1087   and hydrological conditions on the thermal regime of a reservoir at Tropic of Cancer, in
1088   southern China. *Water Research*, *46*(8), 2591–2604.
1089   https://doi.org/10.1016/j.watres.2012.02.014

1090 Wetzel, R. G. (2001). 6 - FATE OF HEAT. In R. G. Wetzel (Ed.), *Limnology (Third Edition)*
1091   (pp. 71–92). San Diego: Academic Press. https://doi.org/10.1016/B978-0-08-057439-
1092   4.50010-1

1093 Wilson, H. L., Ayala, A. I., Jones, I. D., Rolston, A., Pierson, D., de Eyto, E., et al. (2020).
1094   Variability in epilimnion depth estimations in lakes. *Hydrology and Earth System*
1095   *Sciences*, *24*(11), 5559–5577. https://doi.org/10.5194/hess-24-5559-2020

1096 Wu, T., Qin, B., Brookes, J. D., Shi, K., Zhu, G., Zhu, M., et al. (2015). The influence of changes
1097   in wind patterns on the areal extension of surface cyanobacterial blooms in a large
1098   shallow lake in China. *Science of The Total Environment*, *518–519*, 24–30.
1099   https://doi.org/10.1016/j.scitotenv.2015.02.090

1100 Yang, J., Lv, H., Yang, J., Liu, L., Yu, X., & Chen, H. (2016). Decline in water level boosts
1101   cyanobacteria dominance in subtropical reservoirs. *Science of The Total Environment*,
1102   *557–558*, 445–452. https://doi.org/10.1016/j.scitotenv.2016.03.094

1103 Yao, F., Livneh, B., Rajagopalan, B., Wang, J., Crétaux, J.-F., Wada, Y., & Berge-Nguyen, M.
1104   (2023). Satellites reveal widespread decline in global lake water storage. *Science*,
1105   *380*(6646), 743–749. https://doi.org/10.1126/science.abo2812

1106 Ye, Z., Liu, H., Chen, Y., Shu, S., Wu, Q., & Wang, S. (2017). Analysis of water level variation
1107   of lakes and reservoirs in Xinjiang, China using ICESat laser altimetry data (2003–2009).
1108   *PLoS ONE*, *12*(9). https://doi.org/10.1371/journal.pone.0183800

1109 Zhang, M., Zhang, Y., Zhou, Y., Zhang, Y., Shi, K., & Jiang, C. (2022). Influence of
1110   cyanobacterial bloom accumulation and dissipation on underwater light attenuation in a

1111   large and shallow lake. *Environmental Science and Pollution Research*, *29*(52), 79082–
1112   79094. https://doi.org/10.1007/s11356-022-21384-7

1113   Zhao, G., Li, Y., Zhou, L., & Gao, H. (2022). Evaporative water loss of 1.42 million global
1114   lakes. *Nature Communications*, *13*(1), 3686. https://doi.org/10.1038/s41467-022-31125-6

1115   Zohary, T., & Ostrovsky, I. (2011). Ecological impacts of excessive water level fluctuations in
1116   stratified freshwater lakes. *Inland Waters*, *1*(1), 47–59. https://doi.org/10.5268/IW-
1117   1.1.406

1118